

**DANISH METEOROLOGICAL INSTITUTE**  
**TECHNICAL REPORT**

**03-11**

**Evaluation of the AMIS Gridded Observations  
and Radar derived 24-hour Accumulated  
Precipitation by Comparison with Climate Grid –  
Denmark Gridded Observations  
Phase II**

**February 2003**

**Steffensen M.  
Vejen F.**

**ISSN 0906-897X (print) ISSN 1399-1388 (online)**



# Copenhagen 2003

## Preface

This report present results from a project carried out by DMI in 2001 and 2002 as phase II of task number 2 “Forbedrede vejrdata til lokal varsling og beslutningsstøtte for behandlingsbehov mod fugtelskende svampe i korn” in the project “Videreudvikling af beslutningsstøttesystemer” in Pesticide Action Plan II commissioned by the Danish Ministry of Environment and Energy and the Ministry of Food, Agriculture and Fisheries.

The results and recommendations of phase I is described in the Technical Report 01-13: ”Evaluation of the AMIS Gridded Observations and Radar derived 24-hour Accumulated Precipitation by Comparison with Climate – Grid Denmark Gridded Observations”, March 2001.

Phase II follows the recommendations given in phase I.

*DMI, May 2002*

*Michael Steffensen*

*Flemming Vejen*

## List of contents

1.....	<b>Introduction</b>	4
1.1.....	General	4
1.2.....	Methods and Data	4
1.3.....	Outline	5
1.4.....	Abbreviations	5
1.5.....	Glossary	5
2.....	<b>The Field Types</b>	7
2.1.....	CLIMATE GRID - DENMARK	7
2.2.....	AMIS	7
2.3.....	Radar derived 24-hour Accumulated Precipitation	18
3.....	<b>Verification</b>	40
3.1.....	Data	40
3.2.....	Verification Methods	40
3.3.....	Results: Increasing number of observations in the interpolation	40
3.4.....	Results: Radar derived precipitation fields	45
4.....	<b>Conclusions</b>	51
5.....	<b>References</b>	52

## Appendices

- Appendix A: A brief explanation of errors on weather radar data.
- Appendix B: Tables with the overall statistics for 1998 and 1999
- Appendix C: Contingency tables 25 observations in the interpolation 1998
- Appendix D: Contingency tables 62 observations in the interpolation 1998
- Appendix E: Contingency tables 87 observations in the interpolation 1998
- Appendix F: Contingency tables 126 observations in the interpolation 1998
- Appendix G: Contingency tables 25 observations in the interpolation 1999
- Appendix H: Contingency tables 62 observations in the interpolation 1999
- Appendix I: Contingency tables 87 observations in the interpolation 1999
- Appendix J : Contingency tables 126 observations in the interpolation 1999

# **1. Introduction**

## **1.1 General**

The two main tasks of phase II are to study how the field of 24-hour accumulated precipitation in AMIS depends on the number of observation used in the gridding process and to investigate the effect of calibrating the radar derived 24-hour accumulated precipitation using different techniques.

A central component of DMI's AgroMeteorological Information System (AMIS) is the interpolation of observed meteorological data to the 10 by 10 kilometre AMIS grid. The AMIS observational data are generally of high quality (Hilden and Hansen, 1998), however the fields of 24-hour accumulated precipitation tend to be too smooth, not reflecting the fine-scale spatial structure of the actual precipitation fields, probably stemming in part from the quite simple, isentropic interpolation scheme used to calculate the data from the raw observed values, but also from the relative small number of observations involved in the interpolation.

During the spring of 2002 a number volunteer people will read the daily precipitation 8 o'clock in the morning Danish time and report the measurement through telephone to the Danish Meteorological Institute as soon as possible. This will increase the number of available precipitation observations in the AMIS system. When the number of observations is increased the fine-scale spatial structure of the actual precipitation fields is expected to be better represented. This will be demonstrated by comparison of the operational AMIS precipitation pattern on specific day and the precipitation pattern obtained with more observation in the interpolation that day. It has also been investigated how the verification measures depend on the number of observation.

In phase I it has been demonstrated in the case studies that field fine-scale structure was better represented in the radar derived 24-hour accumulated precipitation than in the operational AMIS system. The overall statistical verification measure, such as ME, MAE and HR, on the other hand was not as good as those for the operational AMIS. The aim of phase II was to correct the radar data for anaprop errors and to adjust the radar derived 24-hour accumulated precipitation to get overall statistical verification measure comparable to AMIS.

## **1.2 Methods and Data**

The data sets used in phase II are basically the same as those used in phase I with one major exception. The AMIS data are supplemented with observation from those locations where the additional precipitation observations made available through telephone are expected. These observation are available for the growing seasons 1998 and 1999 though not on daily basis at that time.

### 1.3 Outline

The report is organised as follows:

Chapter 2 contains brief descriptions of the modifications of the operational AMIS field used in this analysis, and the methods of the calibration of the radar data are outlined. The results of the qualitative case studies using the modified methods are discussed. Chapter 3 presents the statistical verification for dependencies on the number of observations used in the interpolation and for adjusted radar derived fields, respectively. Chapter 4 contains the central conclusions. References are given in Chapter 5.

Detailed results of the statistical verification are compiled in an Appendix B to J.

A list of abbreviations and acronyms used throughout the report is given below.

### 1.4 Abbreviations

AMIS	AgroMeteorological Information System, see Chapter 2.2 AMIS.
RADAR	Radar derived 24-hour accumulated precipitation, see Chapter 2.3.
ME	Mean Error, i.e. the sum of the difference between the analysed values and the observations, divided by the number of observations.
MAE	Mean Absolute Error, i.e. the sum of the absolute difference between the analysed values and the observations, divided by the number of observations.
RMSE	Root Mean Square Error, i.e. square root of the mean squared error.
HR	Hit Rate, The sum over each precipitation category of number of correct estimate (AMIS or Radar ) of this category divided by the total number of occurrence in Climate Grid of this category.
HKSI	Hanssen-Kuipers' skill index with climate as reference. HKSI is 1 for a perfect forecasting system and 0 for a "no skill" system. Negative values of HKSI indicates that the forecasting system is inferior to the reference. (Hanssen, A.W., and W.J.A. Kuipers, 1965)

All Hit Rates are given as fractions.

ME, MAE and RMSE are in mm/24hr in tables showing statistics.

### 1.5 Glossary

Anaprop: In meteorological situations associated with nonstandard refraction, strong downward bending of the radar beam may occur leading to echoes from ground targets even far from the radar. This cause spurious echoes. Nonstandard refraction occur when the vertical

distributions of temperature and specific humidity are other than normal.

- Attenuation: The beam power is attenuated due to atmospheric gasses and hydrometeors, i.e. clouds, rain, snow and hail.
- Beam filling: The received power corresponds to the backscattering from a volume of air. If the beam volume is not uniform filled with hydrometeors, e.g. in case of partially filling, representativity problems may arise. The cross section of a radar beam increases with increasing range, thus the problem increases with range.
- Beam power profile: The power profile is the energy level in the beam across the beam axis.
- Bright band: The bright band is the layer in which melting of snow is going on causing a higher reflectivity than in the layers below and above. A thin coating of water results in a very large increase in the reflectivity of a snow sphere due to a larger backscattering cross section.
- Clutter: The reflection of the radar beam from non-meteorological targets.
- Overshooting: The radar beam is situated above the precipitation layer.
- Reflectivity factor: The volumetric integration of the drop diameter in sixth power in the unit  $\text{mm}^6\text{mm}^{-3}$ .
- Refraction: The air-mass properties, i.e. temperature, pressure and humidity, are sufficiently variable to produce small changes in the speed of propagation. This may lead to refraction of the radar ray and produce marked changes in the direction of propagation.
- Sidelobe: The energy is concentrated into a beam along the radar paraboloid axis which is known as the major lobe. Smaller secondary lobes, the sidelobes, are usually found with their central axis directed at various angles with the paraboloid axis.

## **2. The Field Types**

### **2.1 CLIMATE GRID - DENMARK**

A description of climate grid – Denmark is found in the phase I report Technical Report 01-13: "Evaluation of the AMIS Gridded Observations and Radar derived 24-hour Accumulated Precipitation by Comparison with Climate – Grid Denmark Gridded Observations", March 2001.

### **2.2 AMIS**

DMI's operational AgroMeteorological Information System, AMIS, is described in the phase I report Technical Report 01-13: "Evaluation of the AMIS Gridded Observations and Radar derived 24-hour Accumulated Precipitation by Comparison with Climate – Grid Denmark Gridded Observations", March 2001.

#### **2.2.1 Modified AMIS**

In this study four new precipitation fields have been obtained using the same interpolation method as in the operational AMIS, but with a varying number of observations. The total number of available observations is 126 for the Jutland area. Among these observations a subset of 87 observations was randomly chosen in such a way that the coverage has the same degree of homogeneity. The same procedure was performed with 62 and 25 observations.

For each AMIS square, the value at a given time is obtained by a simple distance interpolation with a predefined cutoff radius and weighting with weights proportional to  $d^r$ , where  $d$  is distance and  $r$  is a negative power. The cutoff radius and the power has to be estimated. A small value of cutoff radius will have to few observation in the interpolation and a large value of cutoff radius will include to many observations. An optimum cutoff radius may be found. The power on the other hand is connected to the cutoff radius since a large power will suppress observations at large distances even if the cutoff radius is large.

The cutoff radius and the power is estimated by analysis of the mean absolute error, MAE, of the interpolation of each observation from the others.

For small values of cutoff radius (too few observations) the MAE increases when the power is increased because a large power will reduce the influence of distance observation and thereby further reduce the number of observation in the interpolation.

For a large cutoff radius (to many observations) the behaviour if MAE is opposite. MAE decreases when the power is increased because a large power will reduce the influence of distance observation and thereby reduce the number of observation in the interpolation.

The cutoff radius and the power also depend on the total number of observations available. If the total number of observations is small the cutoff radius has to be large to include sufficient number of observations in the interpolation.

The cutoff radius and the power for each of the four additional fields are listed in table 1.

No of stations	Cut-off radius (km)	Power
25	66	1.5
62	41	1.8
87	36.2	2.0
126	32	1.9

Table 1

## 2.2.2 July 14<sup>th</sup>, 1998: A Cold Front

The synoptic development over Denmark this day is dominated by a low which enters Jutland near Thyborøn and moves eastwards across northern Jutland and Kattegat towards Sweden. During the morning the wind in Jutland is mainly from south to southwest with light showers in the western and southern parts and in Djursland. Strong to heavy showers are reported from Ringkøbing along the west coast to Thisted airport. Light continuous rain in the most southern part of Jutland. A cold front associated with the low reaches Jutland and is at 12:00 UTC stretching from around Mors in the Limfjord southeast across Funen. The synoptic weather map and the position of the cold front at 12:00 UTC are shown in figure 2.1. The wind behind the front is more westerly and light showers prevail across Jutland with still some strong showers on the west coast. At 15:00 UTC the front has moved further eastwards to Kattegat and Sealand and the weather is beginning to clear up in Jutland, though some light widespread showers are still present in Jutland.

Figure 2.2 show the precipitation contours (red curves) for the operational AMIS field together with the contours (blue) of the verifying Climate Grid - Denmark and a scattergram in the lower left corner. The grid precipitation from Climate Grid - Denmark shows up to 15-20 mm of rain at the most wet places. The operational AMIS results show a fairly good correspondence with the wet places in southern Jutland, but a very poor correspondence with wet places in the central and northern Jutland, where the contour lines in many places are even orthogonal.



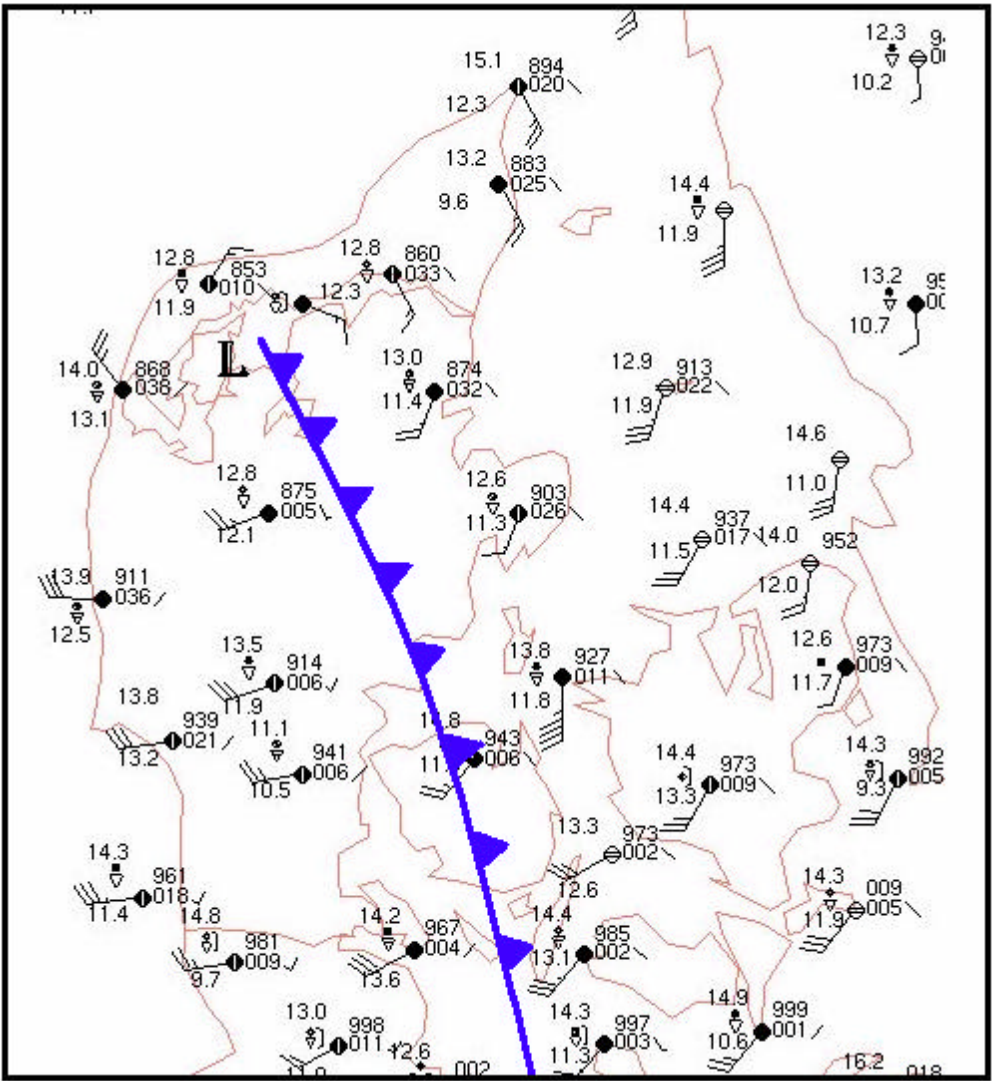


Figure 2.1. Synoptic map for July 14<sup>th</sup>, 1998, 12 UTC.

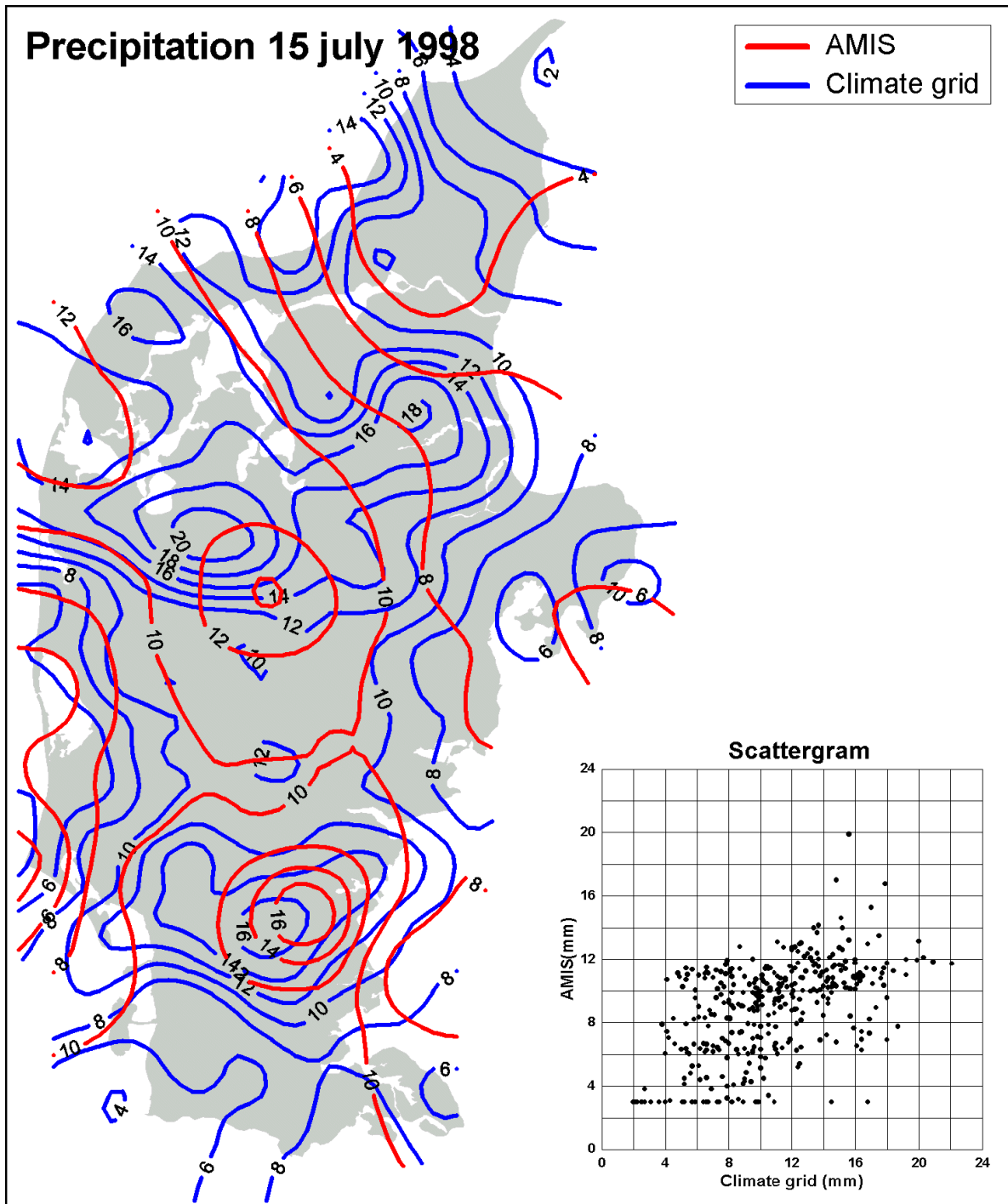


Figure 2.2. Map of precipitation from the operational AMIS for July 15<sup>th</sup>, 1998, 12 UTC, and a scattergram to show the accuracy. This figure is the same as figure 3.5 in Technical Report 01-13: "Evaluation of the AMIS Gridded Observations and Radar derived 24-hour Accumulated Precipitation by Comparison with Climate – Grid Denmark Gridded Observations"

Figure 2.3 shows four precipitation patterns and scattergrams for fields with an increasing number of observations in the interpolation, starting with 25 observation in the upper left corner, 62 observations in the upper right corner, 87 observations in the lower left corner and finally all 126 available observations in the lower right corner

The scattergrams clearly show how the increasing number of observations is reducing the spread in the scattergrams indicating a better retrieval of the fine-scale structure of the precipitation field. In this case however not much is achieved going from 87 observations to 126. The field based on 87 observations captures most of the fine-scale structure, and is much better than the operational AMIS shown in figure 2.2.

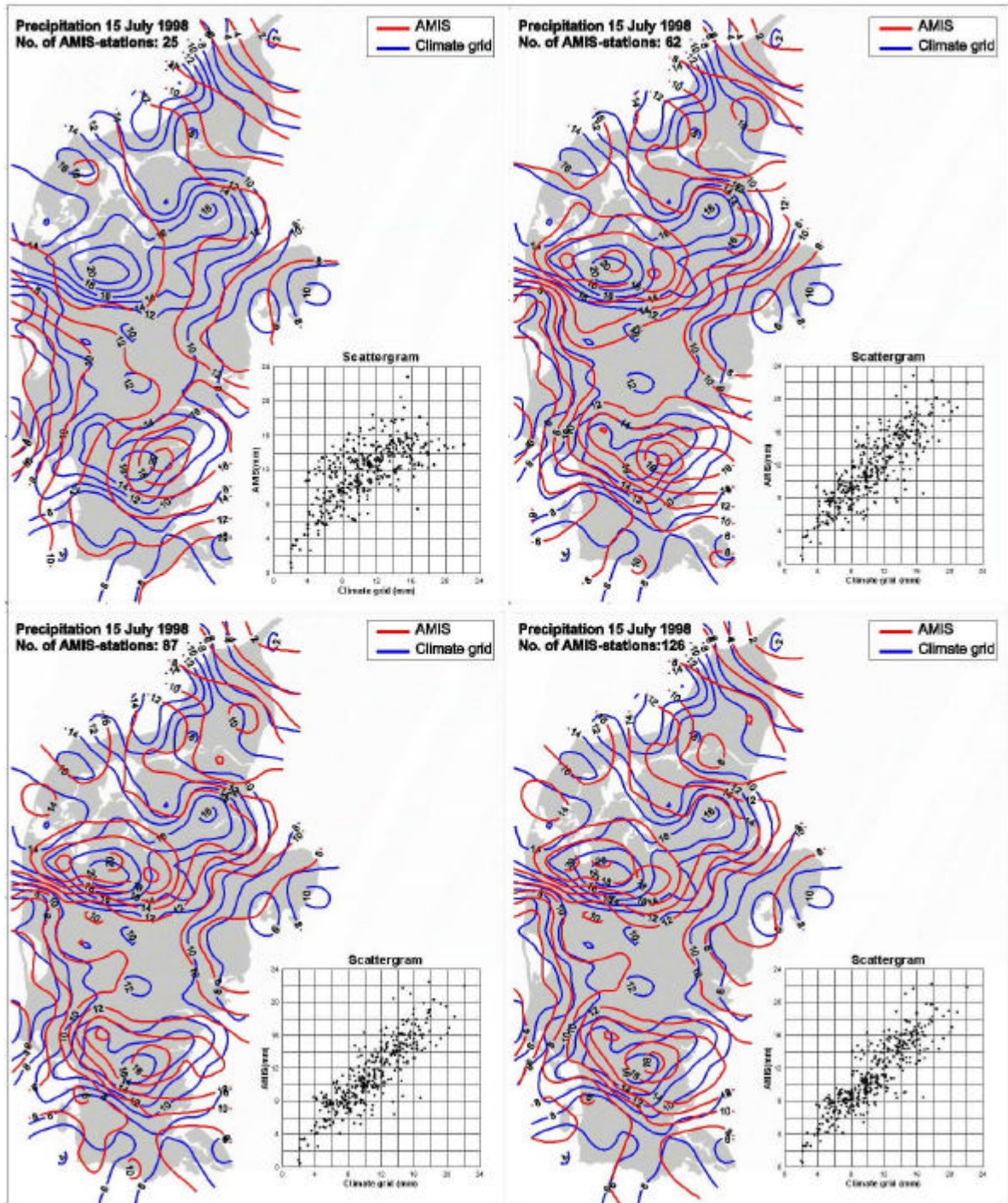


Figure 2.3 Four precipitation patterns and scattergrams for fields with an increasing number of observations in the interpolation, starting with 25 observation in the upper left corner, 62 observations in the upper right corner, 87 observations in the lower left corner and finally all 126 available observations in the lower right corner.

### 2.2.3 June 24<sup>th</sup>, 1999: Showers

The synoptic situation 12 UTC shown in figure 2.4 is dominated by a high pressure area with more than 1020 hPa and a southeast gradient with wind from northwest. This was the general situation during both 24-25 June 1999. Local showers fell mainly in the two areas seen in figure 2.5 showing the precipitation contours (red curves) for the operational AMIS field together with the contours (blue) of the verifying Climate Grid - Denmark and again a scattergram in the lower left corner.

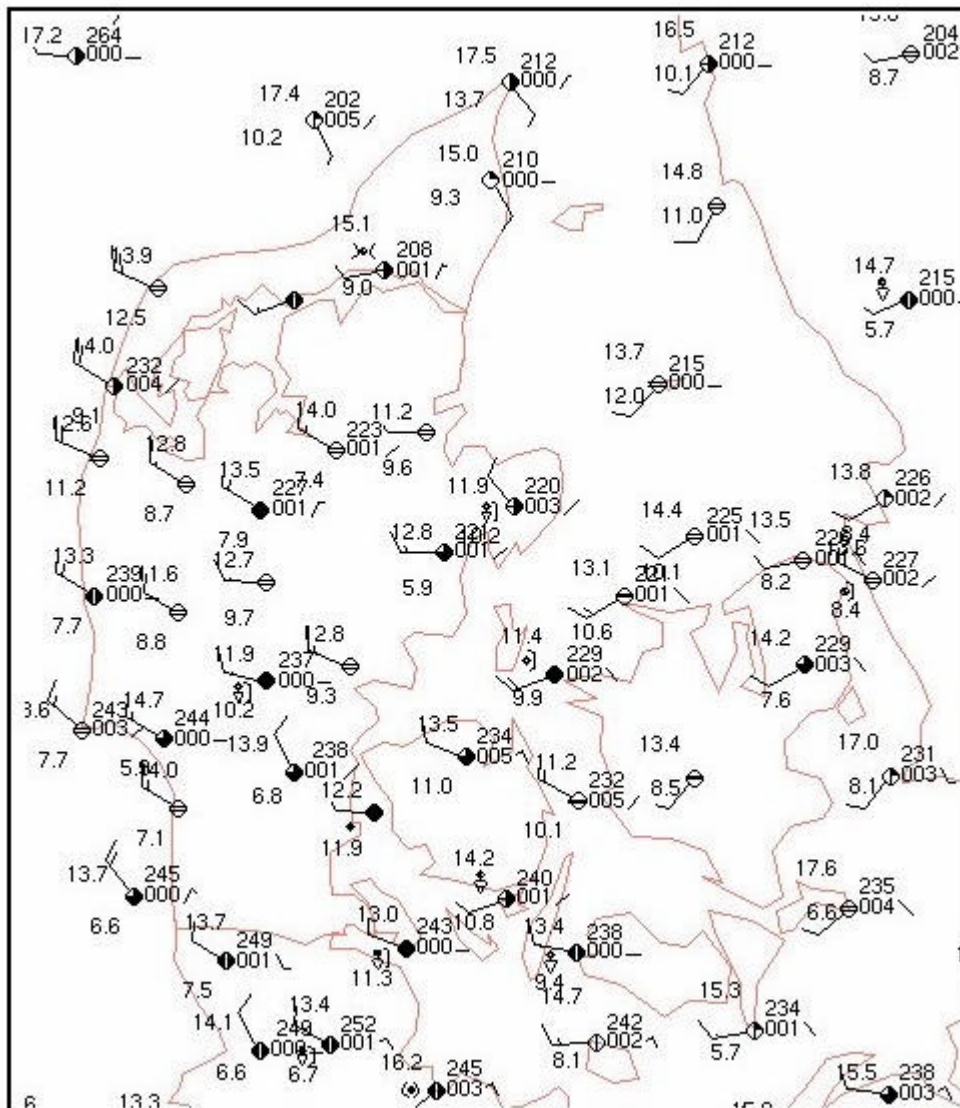


Figure 2.4. Synoptic map for June, 24<sup>th</sup> 1999, 12 UTC.

The operational AMIS field captures to some extent the small precipitation area to the south but completely misses the rather large amount of precipitation, 16 [mm] south of Aalborg. This may also be seen in the scattergram where the AMIS values tend to lie on a horizontal line around 2 [mm] with the Climate Grid values reaching more than 20 [mm].

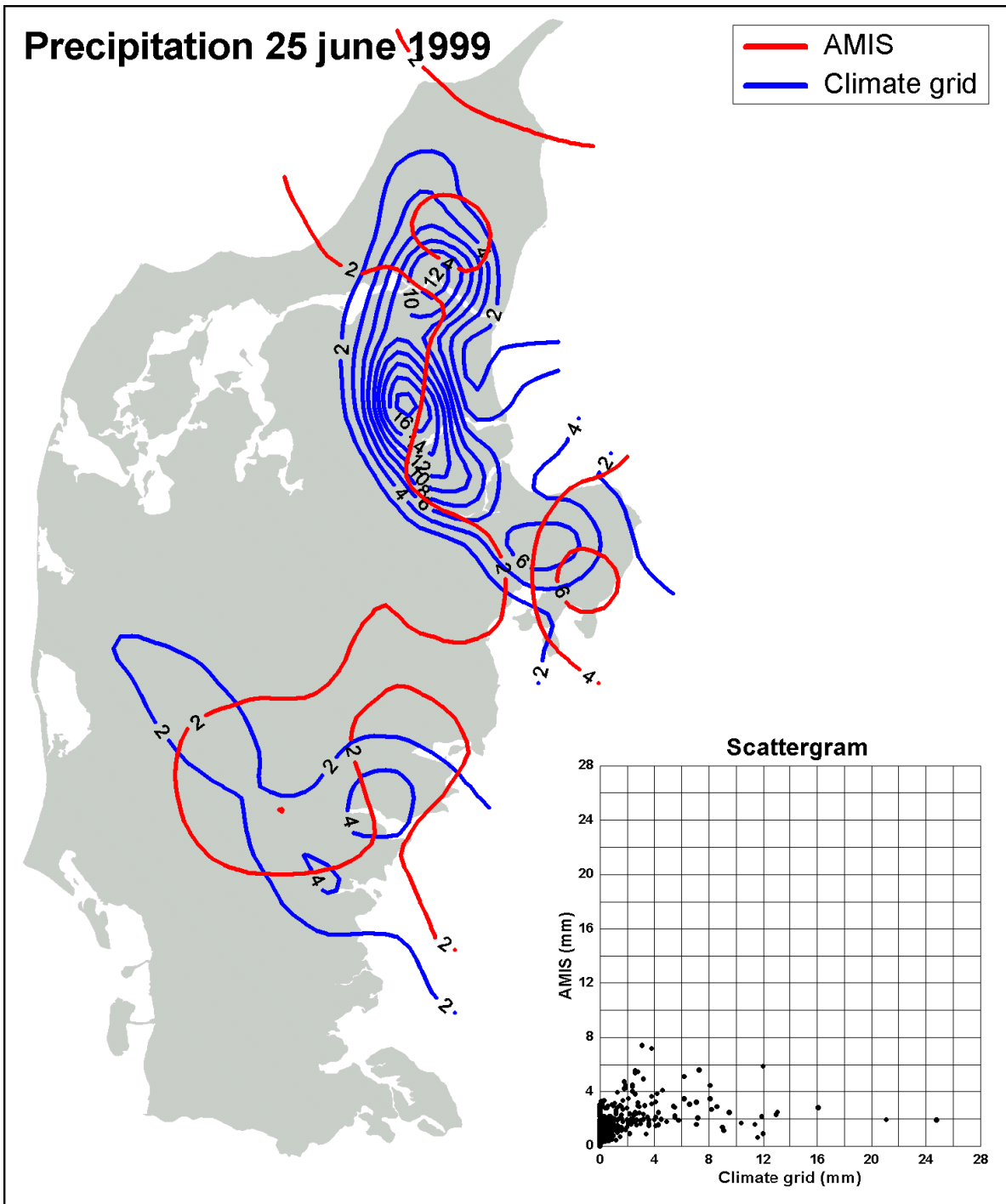


Figure 2.5. Map of precipitation using AMIS for June 25<sup>th</sup> 1999, 12 UTC, and a scattergram to show the accuracy.

Figure 2.6 shows again the four precipitation patterns and scattergrams for fields with an increasing number of observations in the interpolation. Similar to the case 15 July 1998 the precipitation pattern with 87 observations captures both precipitation areas. The scatter in this case however is not so good, which may be due to the rather step gradients in the field. again not much is gained when the number of observations is increased from 87 to 126.

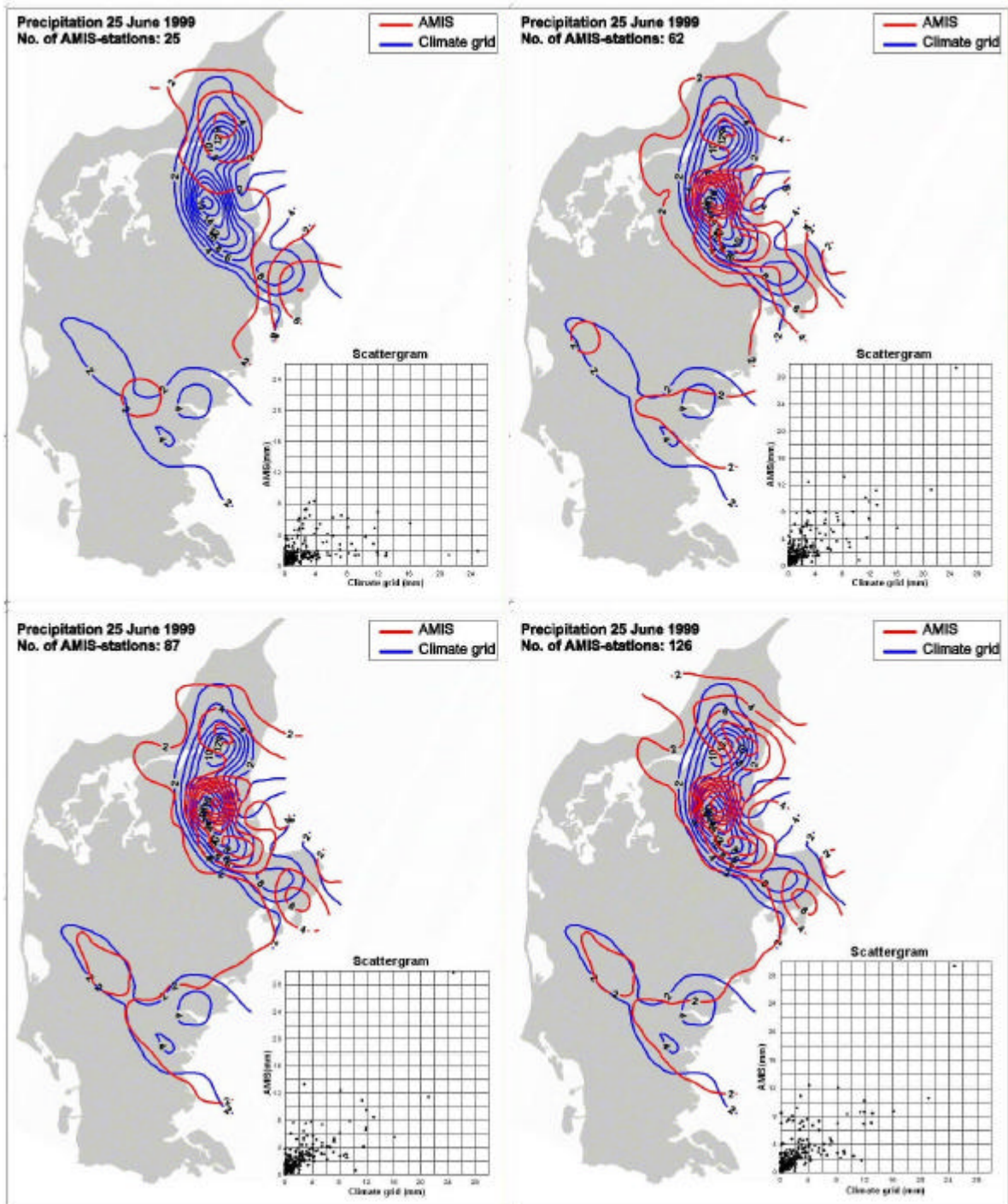


Figure 3.6. Four precipitation patterns and scattergrams for fields with an increasing number of observations in the interpolation, starting with 25 observation in the upper left corner, 62 observations in the upper right corner, 87 observations in the lower left corner and finally all 126 available observations in the lower right corner.

## 2.2.4 August 19<sup>th</sup>, 1999: Heavy Precipitation

During 18-19 August the synoptic situation 12 UTC shown in figure 2.7 is dominated by a high pressure area with more than 1000 hPa and a northeast gradient with wind from south to southeast. The area got widespread and partly heavy convective precipitation, at places quite huge amounts.

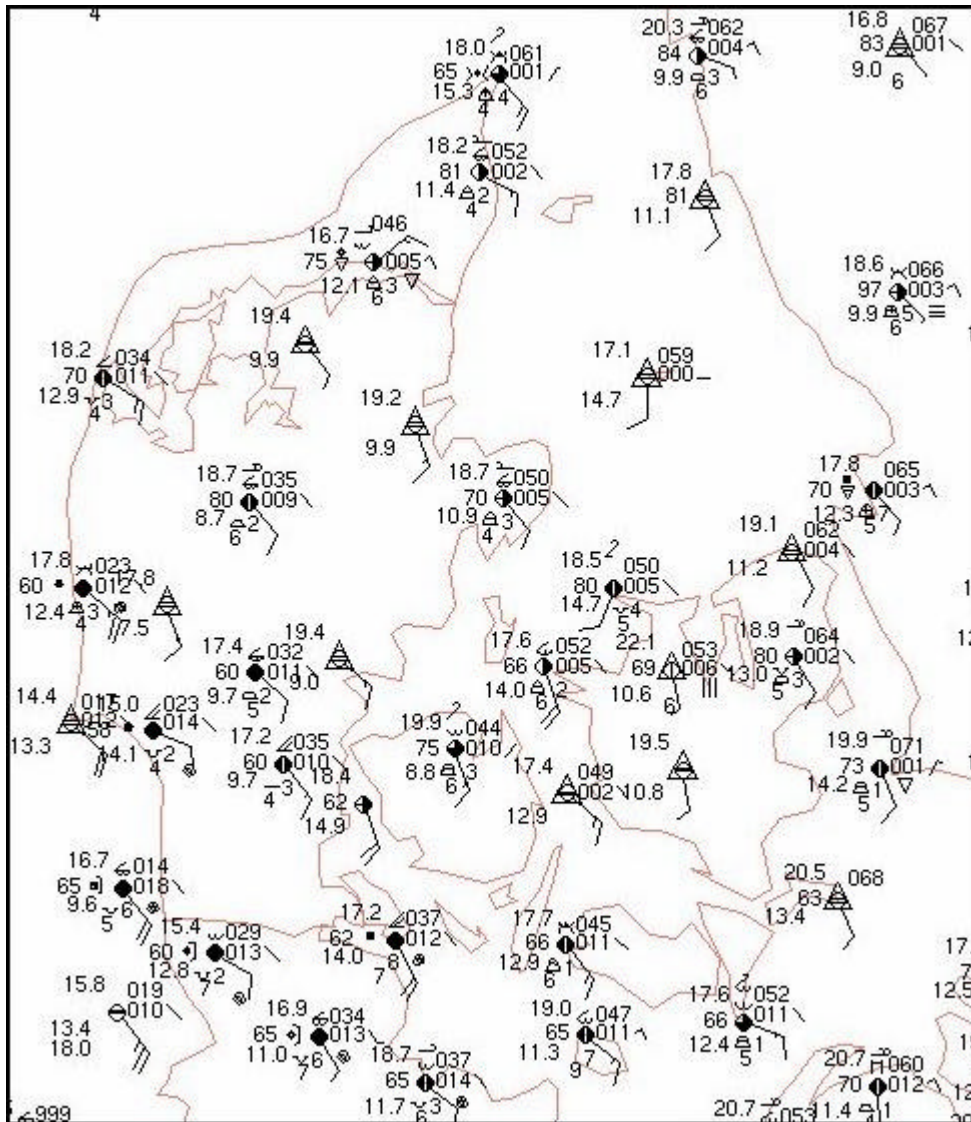


Figure 2.7. Synoptic map for August, 19<sup>th</sup> 1999, 12 UTC.

According to climate grid precipitation there were several precipitation maxima with up to about 30 mm of rain as seen in figure 2.8 showing the precipitation contours (red curves) for the operational AMIS field together with the contours (blue) of the verifying Climate Grid - Denmark and again a scattergram in the lower left corner. Generally, AMIS has difficulties in locating the maximum precipitation correctly. Moreover, the precipitation amounts are very wrong and there are large discrepancies between climate grid and AMIS which can also be seen in the scattergram.

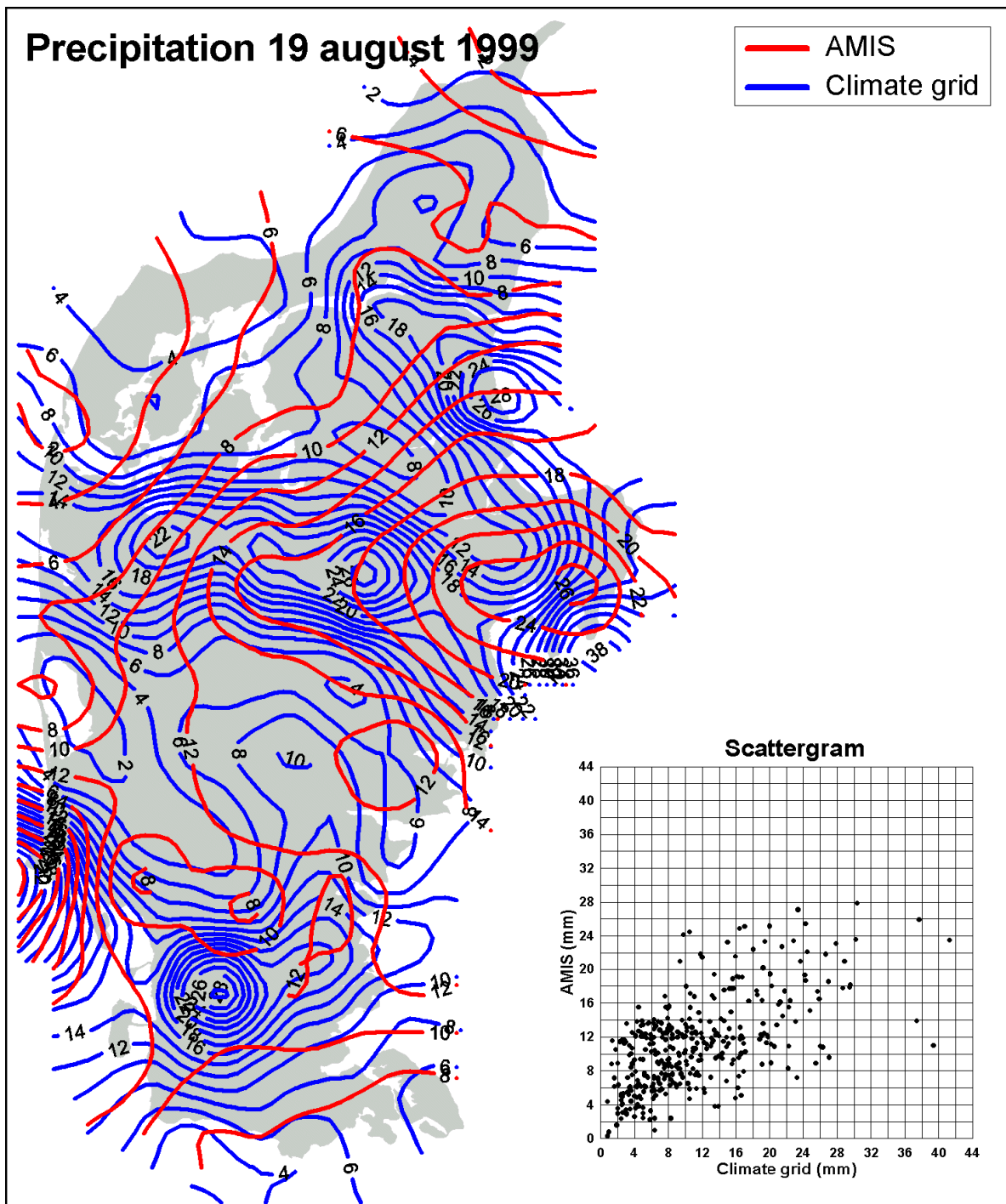


Figure 2.8. Map of precipitation using AMIS for August 19<sup>th</sup> 1999, 12 UTC, and a scattergram to show the accuracy.

The four precipitation patterns and scattergrams for fields with an increasing number of observations in the interpolation shown in figure 2.9 is again demonstrating the increased ability to capture the fine-scale structure as the number of observation is increase. In this case already 62 observations seems to capture the fine-scale structure well, which can also be seen in the



scattergrams where the spread around the identity line looks like a cone structure pointing towards the intersection between the x- and y-axis.

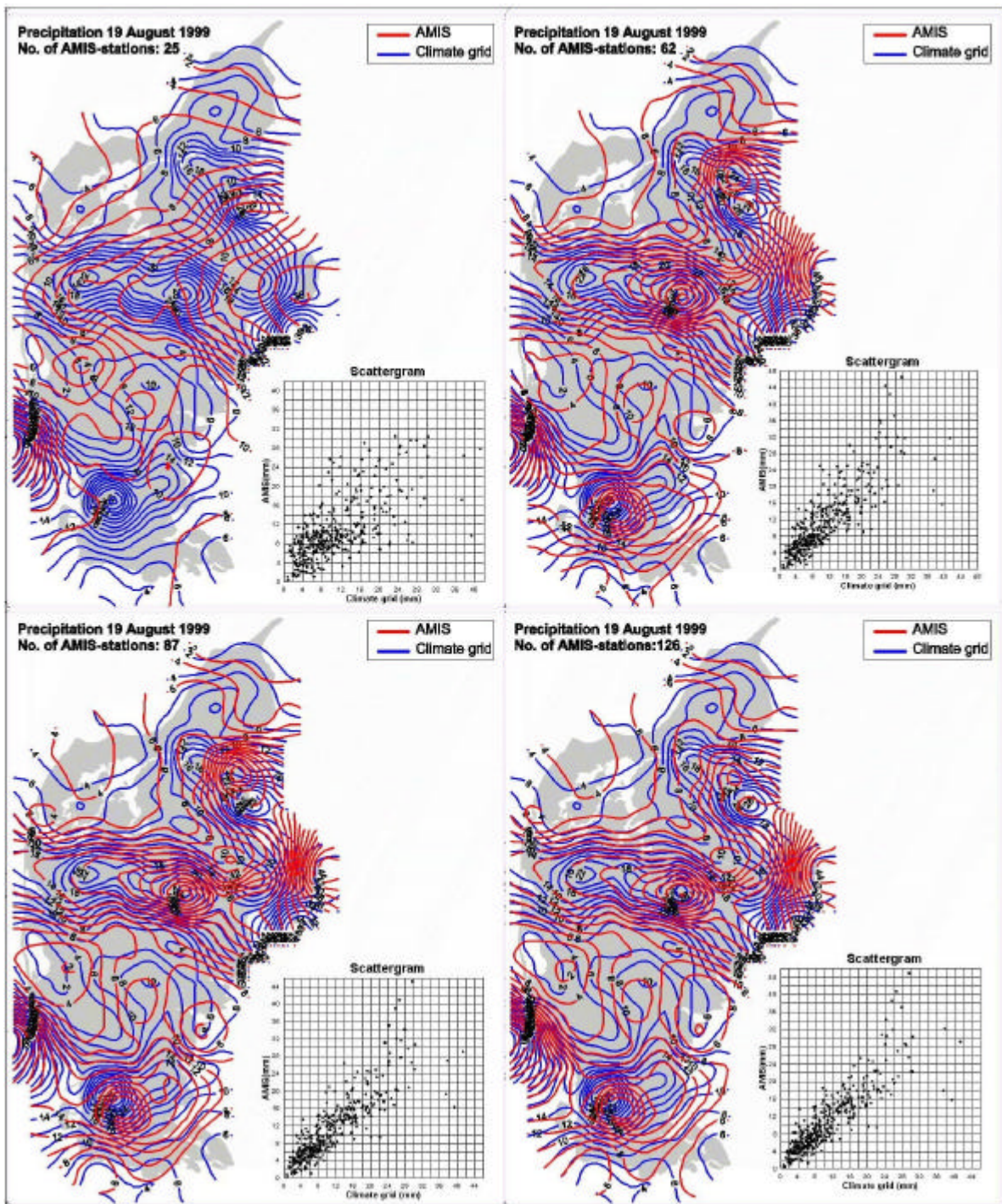


Figure 2.9. Four precipitation patterns and scattergrams for fields with an increasing number of observations in the interpolation, starting with 25 observation in the upper left corner, 62 observations in the upper right corner, 87 observations in the lower left corner and finally all 126 available observations in the lower right corner.

## **2.2.5 Conclusions**

The main conclusion drawn from the case studies is, that increasing the number of observations applied in the interpolation from 25 to 90 is enhancing the resolution of the fine scale structure significantly, whereas increasing the number of observations beyond 90 not much additional structure is gained in the fields. Chapter 3 will illustrate this further using the overall verification statistics.

## **2.3 Radar derived 24-hour Accumulated Precipitation**

In the phase I report: "Evaluation of the AMIS Gridded Observations and Radar derived 24-hour Accumulated Precipitation by comparison with ClimateGrid – Denmark Gridded observations", it was recommended that improvements of radar derived 24-hour precipitation totals could be attained if anaprop infected radar observations were identified and excluded from the analyses. Daily adjustments should be made of radar derived precipitation amounts by using data from raingauge stations. The survey of possible improvements of the AMIS product from the use of radar data is concentrated on these two items.

### **2.3.1 Data**

In a survey on default calibrated radar data against raingauges (Southern Water, 1985), it was shown that the radar performs better than raingauges in frontal situations except at distances up to a few km from the gauges, and in convective events at all ranges except very close to the gauges. To resolve the problem of spatial variations in the adjustment a large number of raingauges are required in the analyses of radar data. Daily precipitation totals from app. 115 raingauge stations have been used out of which 50 stations are full automatic (tipping bucket or weighting type) while the rest are manual stations.

In the analyses are used nearly the same radar data set as in phase I, except that a small number of days has been removed as a result of extended quality control.

### **2.3.2 Pre-processing of radar data**

There are various sources of error on radar data, e.g. anaprop, bright-band effect, vertical reflectivity profile variations, attenuation of the radar beam at range and clutter. Corrections for all known systematic errors on radar data should be applied before any raingauge adjustment (Joss and Waldvogel, 1987).

Correction for beam attenuation, which is due to atmospheric gases and hydrometeors, are carried out to account for the loss of power during propagation of the beam through the atmosphere. Bright-band may lead to big errors on rain rate, up to a factor of five, provided the radar has the necessary spatial resolution to resolve the bright-band layer (Joss, 1990). Corrections for resolving this error should be applied but is not needed because bright-band is normally no problem in the

growth season except in April and early May. Corrections for effects related to vertical reflectivity profile variations, such as the effects of range and orographic enhancement, have not been applied but are only a problem at large range. The correction for clutter uses higher elevation beams close to the radar and filters to remove pixels affected by clutter (for more details, see Steffensen et al., 2001). Biggest problem left is anaprop that is too severe and is not been removed by this method, and efforts have been put to develop a simple approach for identification of anaprop days.

### 2.3.3 Identification of anaprop days

Anaprop is a significant source of inaccuracy on radar derived precipitation sums. Apart from true precipitation, anaprop echoes move in an erratic manner or are stationary. Anaprop is associated with regions of no precipitation at all and is due to temperature and moist inversions during stable weather conditions. The aim of the anaprop identification scheme is to identify: (i) severe anaprop days with spurious radar patterns, and (ii) days where anaprop and precipitation occurs in the same period.

Efforts have been put to investigate if a simple method can lead to substantial improvements of the AMIS results, and the goal is to evaluate the gain by just excluding anaprop contaminated 24-hour periods of radar data. Anaprop days are mostly characterised by large discrepancies between raingauge and radar precipitation totals: while the raingauge totals are close to zero, the radar totals can become extremely high. If there is a good agreement between radar and raingauge totals, anaprop has probably not been present in the 24-hour period.

In order to help the anaprop identification, a ratio F is defined:

$$F = \frac{1}{P} \sum_{n=1}^N \sum_{p=1}^P R_{np(24h)} \bigg/ \sum_{n=1}^N G_{n(24h)}$$

F is the ratio of the sum of the radar totals to the sum of raingauge totals. R=the 24-hour radar total in one pixel at the same position as the raingauge n, G=the 24-hour raingauge total of raingauge n, N=the total number of raingauge stations, and P=the number of pixels being used for estimation of the average radar total at raingauge site n. For description of the method for estimation of R, see chapter 2.3.4 “Procedures for raingauge adjustment”. If no rain has been reported F is undefined, but this has been the case only on three days in 1999.

Figure 2.10 shows a scatter plot of daily radar and raingauge precipitation amounts averaged over the number of raingauge stations. On the most days, there is a quite good agreement between the radar estimates and raingauge values, the radar over- or underestimating by a factor 3 or less in most cases. A large group of points have averaged radar totals much higher than for the raingauges. Probably, these points represent anaprop days.

The idea is that if F exceeds a certain threshold value z there is an increased risk of anaprop contamination within the 24-hour period, and the probability of anaprop, P, is set to a fixed value

1. Then, radar data do not enter the estimation of the AMIS field. If  $F < z$  there is probably no anaprop:

$$P = \begin{cases} 1 & \text{if } F \geq z \\ 0 & \text{if } F < z \end{cases}$$

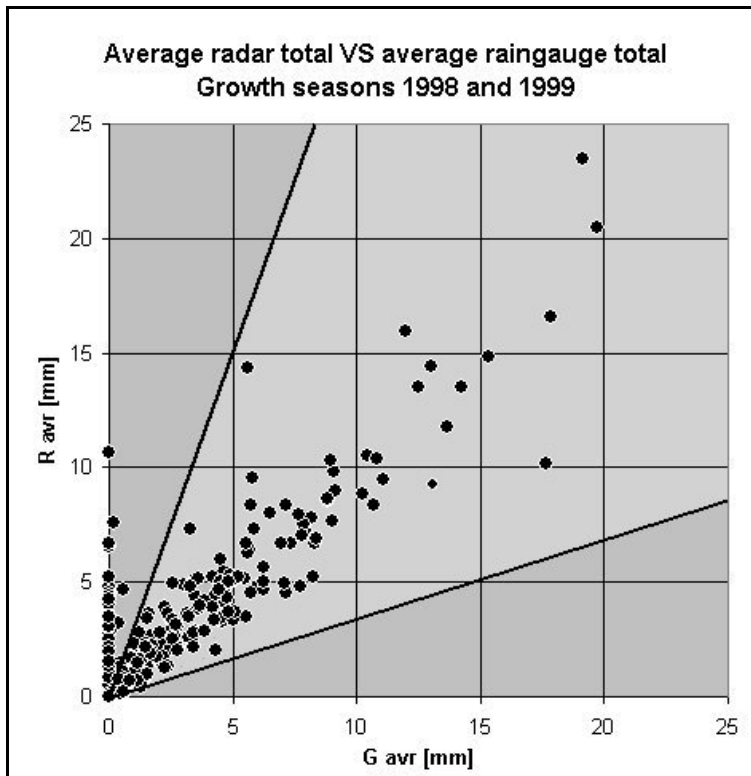


Figure 2.10. Daily precipitation totals for the growth seasons 1998 and 1999 in Jutland averaged over the number of actually reporting raingauge stations, where  $R_{avr}$  is based on from radar data and  $G_{avr}$  on raingauges. The full lines indicate a factor 3 difference between  $R_{avr}$  and  $G_{avr}$ .

In order to verify  $F$  and establish a threshold value  $z$ , it is examined whether  $F$  is a confident measure for identification of anaprop days. On anaprop days, it normally takes some time for widespread frontal rain to enter the area, thus in the most cases only a few or no raingauge stations would be expected to report rain. If they are reporting rain, the amount is probably low. In some cases, severe anaprop and significant rain may hit an area within the same 24-hour period and affect the radar totals deleteriously, and  $F$  should reach high values.

The magnitude and variation of  $F$  is compared with the maximum values of daily raingauge observations and the percentage of raingauge stations with  $>0$  mm (Figure 2.11). For  $F$  values close to one, about 10-100% of the raingauge stations are reporting rain, and anaprop has probably not been present during the 24-hr period. When  $F$  reaches extremely high values most or all raingauge stations are dry, and anaprop is expected. In almost all cases with high  $F$  values, the 24-hour maximum amount of precipitation at the raingauge stations has been less than 1 mm, and for the highest  $F$  values the amount has been very low, 0.2 mm or less.

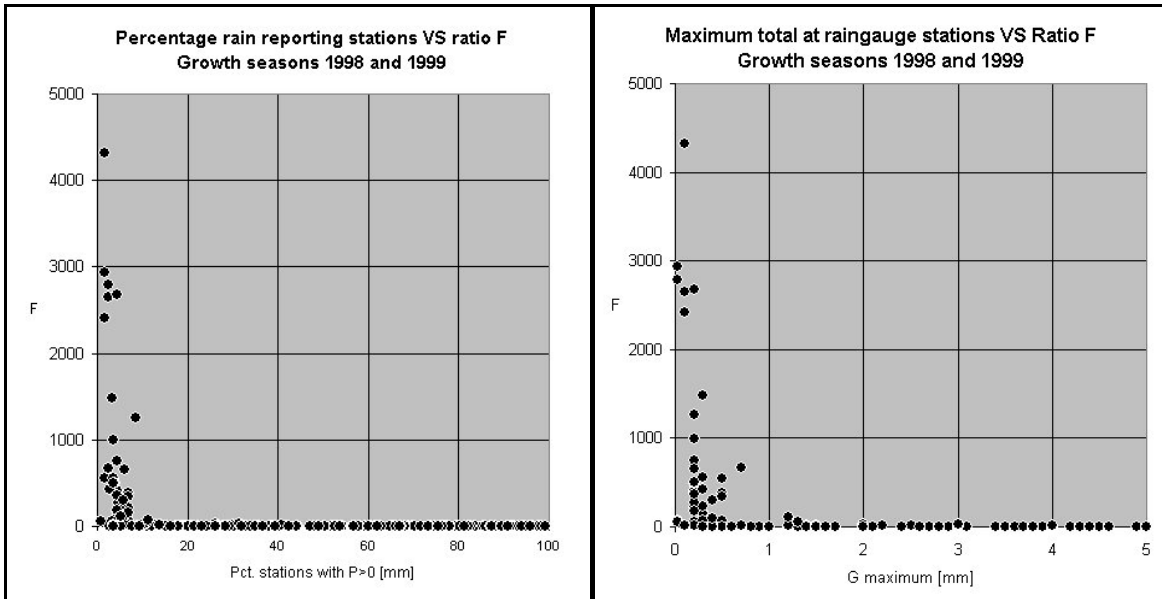


Figure 2.11. Left: scatter plot of F versus pct of stations having more than 0 mm of rain for 1998-1999. Right: scatter plot of F versus mm of rain at the wettest raingauge station for 1998-1999.

Table 2.2 shows the frequency of F in 1998, 1999 and totally together with statistics on gauge totals for various F classes (average and maximum totals, and the percentage of stations reporting rain). Only few or no stations are reporting rain if F has large values. If F=10 it is seen that only 1.5-4.9% of the stations were reporting rain on average, i.e. 2-5 stations. On clear days, trace precipitation (<0.1 mm) or 0.1mm is often reported at manual stations. The reason is nearly always fog or dewdrop accumulation in the gauge leading the observer to report precipitation, and in the whole study period only three days were completely dry at all stations.

F statistics		Intervals for F groups						
		0<F<3	3=F<5	5=F<10	10=F<50	50=F<200	200=F<500	500=F
1998	N	139	12	3	5	4	3	3
1999	N	105	4	7	8	7	9	11
Total	N	244	16	10	13	11	12	14
1998	N%	82.25	7.10	1.78	2.96	2.37	1.78	1.78
1999	N%	69.54	2.65	4.64	5.30	4.64	5.96	7.28
Total	N%	76.25	5.00	3.13	4.06	3.44	3.75	4.38
$G_{avr}$	Avr	3.2176	0.1486	0.1206	0.0448	0.0058	0.0066	0.0035
	max	19.68	0.42	0.57	0.21	0.01	0.01	0.01
	Min	0.00	0.01	0.00	0.00	0.00	0.00	0.00
$G_{max}$	Avr	15.0	3.2	4.0	1.5	0.3	0.3	0.2
	max	84.0	11.0	26.5	6.0	1.2	0.5	0.7
	Min	0.3	0.3	0.2	0.1	0.0	0.2	0.03
%rain	Avr	67.7	25.9	14.2	1.5	4.7	4.9	3.4
	max	99.2	53.0	40.9	31.3	11.2	6.9	8.5
	min	2.6	6.9	3.4	3.4	0.9	2.6	1.7

Table 2.2. Statistics of various F classes are shown for 1998, 1999 and totally. N=total number of days, N%=percentage of days in a F group,  $G_{avr}$ =daily raingauge totals averaged over all stations,  $G_{max}$ =daily maximum if raingauge totals, and %rain=daily percentage of stations reporting rain.

According to Table 2.2, app. 81% of all days in 1998 and 1999 had reasonable F values ( $<5$ ), but 10-15% of the period may have been contaminated by anaprop. Moreover, anaprop was much more frequent in 1999 than in 1998. Normally, the weather conditions during anaprop are stable and persistent, and frontal rain systems are often weakened and moving slowly when approaching. In fact, widespread rain did not occur together with severe anaprop within the same 24-hour period in 1998 and 1999.

Only in a few cases, isolated showers or weak fronts occurred together with anaprop, but then  $G_{\max}=0.5$  mm was measured even in case of very high F values. In the most cases, F is well below 10, and  $F<3$  are always associated with rain. This argues  $F=3$  to be chosen as the threshold value Z.

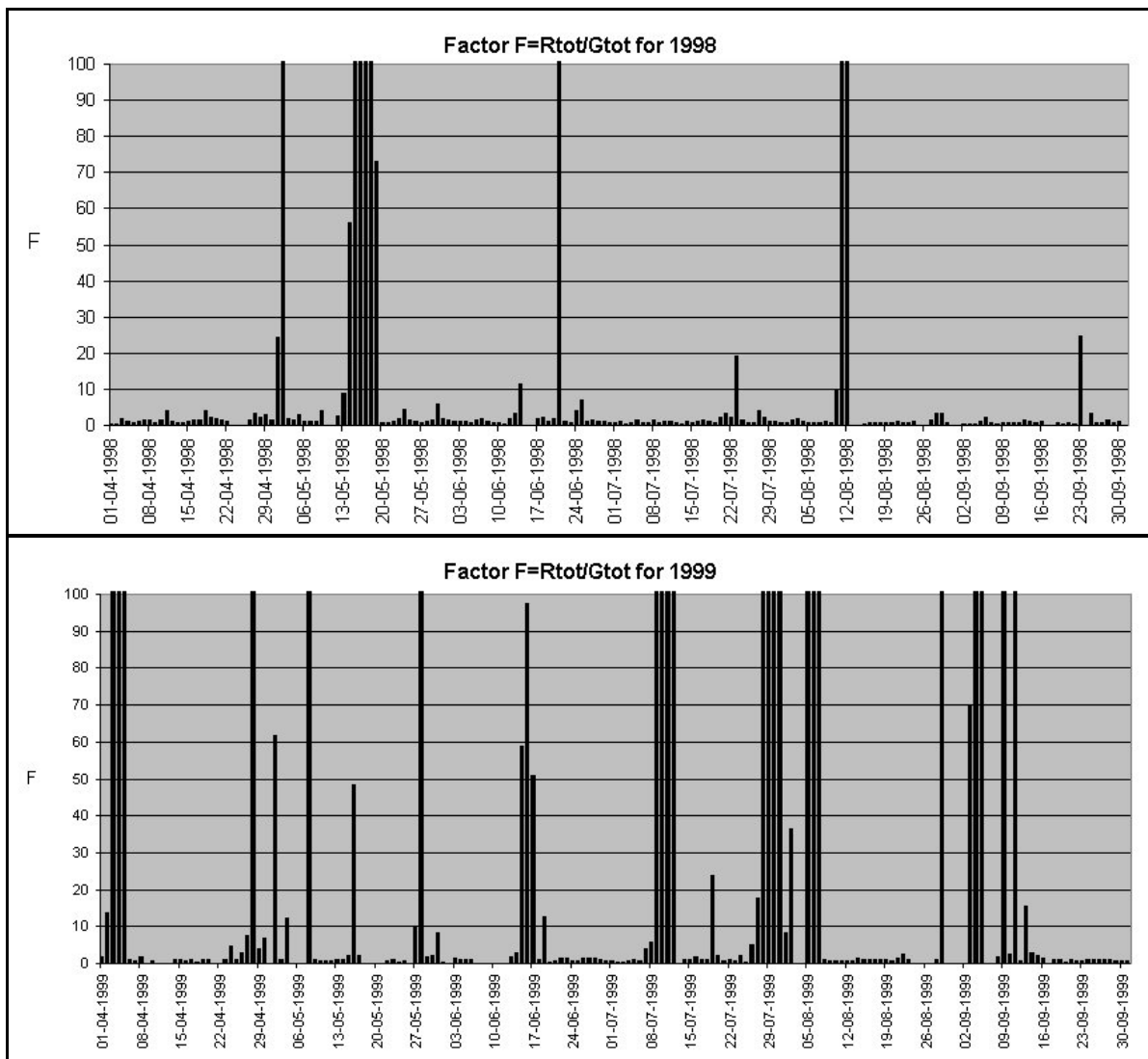


Figure 2.12. The magnitude of the ratio F during the growth seasons 1998 and 1999. On several days, F was much larger than 100, in few cases more than 1000, but the y-axis has been cut off to show small F values.

The day-to-day variations of  $F$  can be very large (Figure 2.12) and the absolute value of  $F$  is often extremely high. The y-axis is cut off at  $F=100$  to accentuate small values of  $F$ . Of no doubt, days with large  $F$  values do have serious anaprop and it is not recommended to let the radar rain totals enter the AMIS system. In order to verify the results of the analyses of  $F=10$  by independent information, 24-hour sequences of radar images have been subject to subjective assessment in order to classify them according to the intensity of anaprop. The persistency of anaprop is not considered. The detailed results in Table 2.3 are summarised in Table 2.4.

Table 2.3(a). Statistics for days with F=10 for the growth seasons 1998-1999 sorted by increasing F value. N=number of raingauge stations. N>0: number of raingauge observations with rain or tracer (<0.1mm). G<sub>max</sub>=largest amount of precipitation at the raingauge stations. R<sub>max</sub>=highest amount of precipitation according to the radar. ? G, ?R =rain total at the raingauge stations and radar, respectively. F=ratio between radar and raingauge totals. A<sub>rømsø</sub> and A<sub>sindal</sub>: classification of anaprop contamination for a 24-hour sequence of radar images, where 0=no anaprop, 1=patches of anaprop, 2=quite strong anaprop, but land contour is not seen in radar images, 3=severe and widespread anaprop, land contour is evident in radar images. The date indicates the 24-hour period since the previous day. (Table continues on next page...)

Date	N	N>0	G <sub>max</sub>	R <sub>max</sub>	? G	? R	F	A <sub>rømsø</sub>	A <sub>sindal</sub>	Comments
15-05-1998	117	2	0.1	73.3	0.1	561.0	4315.0	3	3	Fog reported
11-09-1999	116	2	<0.1	44.7	0.1	176.4	2940.5	2	2	Fog reported
28-04-1999	115	3	<0.1	35.7	0.1	251.1	2790.1	3	3	Some fog reported, few clouds
30-07-1999	116	5	0.2	210.7	0.5	1233.6	2681.8	3	3	Fog reported
29-07-1999	116	3	0.1	139.0	0.2	608.4	2645.1	3	3	Fog reported
08-05-1999	116	2	0.1	49.3	0.1	313.7	2412.9	0	3	Small shower lines in the beginning
05-08-1999	117	4	0.3	133.9	0.5	784.3	1479.9	3	3	Fog reported
18-05-1998	117	10	0.2	198.8	0.6	767.2	1257.6	3	3	Fog reported
03-04-1999	116	4	0.2	96.4	0.5	526.3	993.0	3	1	Nearly cloudless
02-05-1998	117	5	0.2	172.4	0.6	419.1	748.3	3	3	In the North rain in the beginning
31-07-1999	116	3	0.7	110.5	0.8	508.5	669.0	3	2	Fog reported
05-09-1999	116	7	0.2	63.0	0.6	402.1	648.5	3	3	
11-07-1999	116	4	0.3	53.7	0.5	293.5	553.8	3	3	Fog reported
10-07-1999	116	2	0.5	47.8	0.5	290.7	548.5	2	2	Fog reported
04-09-1999	115	4	0.2	98.1	0.4	178.9	497.0	2	2	Fog reported
12-07-1999	52	2	0.2	24.8	0.2	113.1	491.7	no data	3	
28-05-1999	114	3	0.3	33.6	0.4	151.9	422.1	3	1	Fog reported
04-04-1999	116	5	0.2	63.5	0.6	229.7	410.2	2	1	
11-08-1998	116	8	0.5	105.1	1.2	466.5	382.4	2	3	Anaprop and rain in same images
21-06-1998	116	5	0.2	76.4	0.5	186.4	380.4	3	1	Fog and drizzle reported
28-07-1999	116	5	0.2	48.2	0.6	227.5	361.1	2	2	
06-08-1999	118	8	0.5	124.9	1.5	500.1	335.6	2	3	Showers in the beginning
07-08-1999	52	3	0.4	48.6	0.5	158.0	298.1	no data	2	
09-07-1999	65	3	0.2	16.6	0.6	163.0	271.6	3	no data	
05-04-1999	116	6	0.3	22.5	0.8	179.0	235.5	1	2	



Table 2.3(b). (... Table continued). See table text on previous page for explanation.

Date	N	N>0	G <sub>max</sub>	R <sub>max</sub>	? G	? R	F	A <sub>rømsø</sub>	A <sub>sindal</sub>	Comments
17-05-1998	117	8	0.2	31.4	0.7	151.9	211.0	2	2	Fog reported
29-08-1999	117	5	0.2	14.6	0.3	58.2	181.8	1	1	A shower in the beginning
16-05-1998	117	5	0.3	45.5	0.8	127.9	168.3	2	2	
12-08-1998	116	8	0.3	15.7	0.6	88.2	152.0	2	3	Anaprop and rain in same images, fog reported
09-09-1999	115	6	1.2	65.2	1.4	153.2	107.9	1	2	Local rain
16-06-1999	117	5	0.4	21.9	0.9	83.8	97.4	2	0	Fog reported
19-05-1998	117	8	0.5	8.5	0.8	57.1	73.2	2	2	Fog and local drizzle reported
03-09-1999	116	13	0.3	23.4	1.3	93.4	69.7	2	1	Showers in the beginning (rain, drizzle and fog reported)
02-05-1999	116	1	<0.1	1.0	<0.1	1.9	61.7	0	0	Local fog reported
15-06-1999	117	1	<0.1	0.7	<0.1	1.8	58.7	1	0	Fog reported
14-05-1998	117	4	0.2	5.0	0.6	35.4	56.2	0	1	Isolated showers, fog reported
17-06-1999	117	4	0.2	7.6	0.7	35.6	50.9	1	0	
16-05-1999	116	5	1.3	29.3	1.5	72.0	48.3	1	2	Rain in the beginning, fog reported
02-08-1999	118	13	6.0	139.1	24.6	899.5	36.6	3	3	Cb's with rain and thunder
23-09-1998	115	36	0.3	88.5	5.3	130.4	24.6	1	3	Showers in the beginning
01-05-1998	115	30	2.0	110.3	14.0	341.5	24.4	2	1	Rain in the beginning, otherwise anaprop
19-07-1999	116	12	3.0	33.0	4.9	116.4	23.7	2	0	Showers in the beginning
23-07-1998	116	7	0.3	2.2	0.7	13.4	19.3	1	1	Isolated showers
27-07-1999	116	5	0.3	2.9	0.5	8.7	17.8	1	0	Isolated showers in the South, local fog reported
13-09-1999	116	4	0.1	2.3	0.3	4.0	15.4	0	0	Local fog reported
02-04-1999	116	7	1.4	6.6	3.3	46.0	13.8	1	1	Nearly cloudless
19-06-1999	117	7	0.2	3.7	0.8	10.0	12.6	1	0	
04-05-1999	116	8	1.2	22.5	3.0	36.7	12.3	0	1	Shower lines
14-06-1998	116	15	1.4	12.8	5.6	63.5	11.4	1	0	Small showers in the beginning
10-08-1998	116	12	2.2	3.9	3.1	31.2	10.0	1	2	Anaprop in the North, in the beginning rain in the South
05-05-1999	116	0	0	-	0.0	24.8	-	0	2	Cloud streets, isolated showers
06-05-1999	116	0	0	-	0.0	5.0	-	0	1	
07-05-1999	67	0	0	-	0.0	1.2	-	0	no data	

Four anaprop classes are defined: for the classes 2 and 3 anaprop is severe and widespread, and in class 3 land contours and coast lines are clearly seen, but not in class 2. In class 1 only patches of anaprop occurs, and in class 0 no anaprop is present at all.

$R_{max}$  is extremely high compared to  $G_{max}$  in most cases, especially for large F values, and is associated with severe anaprop in the Rømø or Sindal radar area, or the both. Sometimes, rain or tracer precipitation (<0.1mm) has been reported, but it is caused either by dewpoint accumulation, or by weak fronts and isolated showers entering the area during the period. For example, on the 4-5th of May 1999, very isolated showers were present according to the radars, but at the same time the raingauge stations did not report any rain at all, and later on quite severe anaprop popped up in the Sindal radar area. On the 2nd of August 1999, a few quite heavy showers were present in the radar images. A few weather stations were reporting Cb clouds with rain and thunder, and one station got 6.0 mm. In the same 24-hour period severe anaprop was present (anaprop class 3). The reported rain totals caused F to be only 36.6, but anyway it indicated that something spurious was going on. The examples show that even though true radar rain areas are present in the images, they should not enter AMIS if anaprop is present.

Now is left to answer the question how many of the anaprop days had true precipitation (Table 2.4). For increasing anaprop classes the average value of F and the number of occurrences in higher F classes increases. The number days with severe anaprop (class 2 and 3) and radar rain echoes during the same period were only 6 out of 22, and only two anaprop days had significant precipitation with one or more stations reporting >0.5 mm. The rain echoes were corresponding to isolated showers in almost all cases.

Anaprop Class	N(P=0)	N(P>0)	N(P>0.5)	F <sub>avr</sub>	F categories							
					10-19	20-49	50-99	100-299	300-499	500-999	=1000	
0.0	2	0	0	38.5	1		1					
0.5	3	4	2	31.4	4		3					
1.0	2	3	1	67.2	2	1	1	1				
1.5	3	5	3	414.9	1	2	1	2	1			1
2.0	11	1	0	576.5		1	1	3	4	2		1
2.5	1	3	1	384.8				1	2	1		
3.0	10	2	1	1493.3		1		1	1	3		6

Table 2.4. Statistics on 24-hour radar image sequences sorted by anaprop class (for definition, see text). The table shows the number of sequences in different F classes and precipitation classes N. N(P=0): number of completely dry images sequences. N(P>0): number of sequences in which rain echoes have been observed. N(P>0.5): number of sequences in which radar rain echoes have been observed and more than 0.5 mm has been reported from at least one raingauge station. F<sub>avr</sub>=average F value for all sequences in an anaprop class.

### 2.3.4 Procedures for raingauge adjustment

For adjustment of radar derived 24-hour accumulated precipitation a system is developed. Because there seems to be case-to-case variations in the errors on radar data, particularly at long range, only raingauges within certain ranges should be used (Kitchen and Jackson, 1993). Simple comparisons between gauge and radar at long range may not reflect the true rain rate underestimation by radar because of the detection failures of the radar (Kitchen and Jackson,

1993), thus, according to experience only raingauges up to 100 km's distance enter the adjustment scheme to avoid that vertical reflectivity profile problems at range influence the adjustment.

The energy of the returned radar beam power reflected from hydrometeors in a volume of air depends on the drop diameter  $D$  in sixth power and the number of drops  $N$ . The reflectivity factor  $Z$  is estimated from the returned power, which the radar measures.  $Z$  depends on the drop size distribution and thereby the precipitation type, and it is related to rain rate  $R$  (mm/hr) by  $Z$ - $R$  relationships of the general form  $Z=AR^b$ , where  $A$  and  $b$  are empirical constants (e.g. see Battan, 1973). Knowing that the value of  $Z$  is proportional to the number of drops in first power but the drop diameter  $D$  in sixth power, the reflectivity factor  $Z$  reaches, for the same rain rate, large values in convective precipitation and small values in drizzle because the number of large drops is much larger in convective precipitation than in drizzle.

The best way of comparing results is to make sample sizes of radar and raingauges as similar as possible by integrating the linear quantity of interest in time and space. The integration is done in rain rate, not in reflectivity, as recommended by Joss (pers. comm.). The 24-hour amount of rain,  $R'$ , is estimated firstly by integrating every radar image (pseudo-CAPPI image) in rain rate units over all 10-minute pixels,  $i$ , by using a standard  $Z$ - $R$  relation valid for widespread rain (Marshall-Palmer, 1948):

$$R' = \frac{1}{P} \sum_{i=1}^N \sum_{p=1}^P d_i \cdot (Z_{ip} / A)^{1/b}$$

$A=220$ ,  $b=1.60$ ,  $d$ =a time correction factor which is estimated from the actual temporal resolution of the radar images,  $P$ =the number of pixels in a matrix  $J \times J$  around the raingauge location, and  $N$ =the number of images.

Secondly, the accumulated radar totals are adjusted by using the most appropriate adjusting formula for the day in question, and, finally,  $10 \times 10 \text{ km}^2$  grid cells are estimated on the basis of the 24-hour adjusted precipitation sum image.

Weather radars are quite accurate in measuring the extent of a rainfall area, but bias may arise if large differences exist between the standard  $Z$ - $R$  relationship used and the actual  $Z$ - $R$  conditions. The raingauge adjustment scheme focuses on reduction of systematic variations and residual errors in radar rain amount, and the adjustment domain is the whole area of radar coverage. Because it is a procedure designed to work in near real-time, it must respond to daily changes, but a sampling period must not be too short as to introduce sampling errors (Collier, 1987). The radar and raingauge total is integrated over 24 hour because the fact that most manual stations are measuring only once a day.

The adjustment scheme consists of 3 steps:

- *Step 1*: Estimation of the actual  $Z$ - $R$  relationship.
- *Step 2*: If step 1 fails, estimation of a calibration factor **m**.

- *Step 3:* If step 2 fails, a standard Z-R relationship is applied.

In step 1, a regression method is used which works in a spatial-temporal domain. The actual Z-R relationship is estimated on the basis of statistical analyses of 24-hour integrates of Z and R. The Z-R relation is evaluated by correlation analysis, tests of significance and estimation of error statistics, and it is assessed whether the constants A,b in  $Z=AR^b$  attains realistic values. Numerous Z-R relationships have been derived (Battan, 1973), but almost no effort has been put to the calculation of R-Z relationships, i.e.  $R=(Z/A)^{1/b}$ . Stout and Mueller (1968) argued that Z should be the independent parameter in the correlation of the logarithms of R and Z. Even if the correlation coefficient is larger than 0.9 the use of Z-R relationships instead of R-Z may cause errors in R of up to 50% (Kreuls, 1991). Therefore, R-Z relationships enter the adjustment scheme.

In certain weather situations the actual Z-R relationship does not lead to significant reduction of the bias between the radar and the raingauge totals, or any significant Z-R relationship may not be found, or A,b do not attain realistic values (rejection reasons, see Table 2.5). In that case, a simple adjustment method is applied to step 2. It is based on simple deterministic principles by which an adjustment factor derived from temporally and spatially integrated values of G and R' is defined as  $m = G_n / R'_n$  that is applied to the default calibrated radar image.  $G_n$ =the raingauge accumulation at station n, and  $R'_n$ =the default adjusted radar sum at gauge position, where G is assumed to represent the true precipitation. By this mean the effect of adjustment should be to try and minimise the errors in area accumulations, which would tend to be dominated by low rainfall rates if factor **m** just was calculated as an average G/R' ratio.

Step 1	Step 2
no raingauge data and/or no radar data available	
Ttest failure on 5% level	factor m out of bounds: $m < 0.3333$ or $m > 3$
bad A constant: $A_z > 999$ or $A_z < 50$ or $A_r < 0$	
bad b constant: $b_z > 2.49$ or $b_z < 1.10$ or $b_r < 0$	too low G or R' totals: gauge total ? $G < 5$ or radar total ? $R' < 5$
skew adjustment Z, unrealistic(Z): $R_{\min(Z)} = (Z/A_z)^{1/b_z} = 0.05$ , where $Z=0.25$ is set	
Skew adjustment R,unrealistic(R): $R_{\min(R)} = (Z/A_r)^{1/b_r} = 0.05$ , where $Z=0.25$ is set	too few wet obs: $n < 20$
Rrad adjustment problems	

Table 2.5. Reasons for rejection of the Z-R relationship in step 1, and for rejection of the adjustment factor in step 2.

If step 2 fails, e.g. because the number of Z-R data pairs is too small or the adjustment factor is supposed to be unrealistic large or small (see Table 2.4), a standard Z-R relationship is used instead, which is the Marshall-Palmer equation  $Z=220R^{1.60}$  for widespread rain (Marshall and Palmer, 1948).

### 2.3.5 General results

Table 2.6 shows the overall performance of the radar adjustment scheme. On approximately 31% of all days in the growth seasons 1998 and 1999, it was possible to estimate an actual Z-R relation that in fact was able to improve the estimates of radar rain totals. For various reasons, this was not possible in the rest of the growth seasons. The reasons for this are summarised in the table. In many cases, the empirical constants A and b were not realistic because they attained too high or low values. In other cases, the relationship between Z and R was not significant, or R' attained unrealistic values.

Number of adjustments				
	1998	1999	Total	Total %
Actual Z-R relation	53	47	100	30.9
Adjustment factor m	73	66	139	42.9
Standard adjustment Z-R	43	42	85	26.2
Total	169	155	324	100.0
Rejection reasons for actual Z-R relation				
Unrealistic value of b	16	14	30	13.4
Unrealistic value of A	48	46	94	42.0
R' adjustment problems	38	35	73	32.5
Unrealistic value of R'	9	8	17	7.6
T test failure	5	5	10	4.5
Total	116	108	224	100.0
Rejection reasons for adjustment factor m				
? G, ? R totals are too low	21	20	41	48.2
Factor m out of bounds	20	20	40	47.1
too few observations of rain	2	2	4	4.7
Total	43	42	85	100.0

Table 2.6. The table shows the overall performance of the adjustment scheme by statistics on the number of adjustments being done by actual Z-R relations, adjustment factor m and standard adjustments Z-R. It also shows statistics on the number of various reasons of rejection of the two adjustment methods

Nevertheless, it is a quite good result that it was possible to calculate a Z-R relation in about one-third of all days during 1998 and 1999. In case of Z-R failure, the more simple adjustment factor method is applied for estimation of radar totals. This method accounts for about 43% of all adjustments. The most common reasons for failure of this method are that the adjustment factor **m** is out of bounds, or that the amounts of rain is very small so that problems would probably arise if the adjustment factor were applied. When **m** is out of bounds, the reason is probably presence of anaprop during the period, i.e. the ratio F attains very high values. If ? G is very small, anaprop may also be present, and if both ? G and ? R' is very small the adjustment factor is probably not representative of the rain area.

Finally, if the above methods fail a standard Z-R relation is applied. This happened in 26% of all occurrences.

The scatter plots in Figure 2.13, 2.14 and 2.15 shows the overall performance of the actual Z-R relationships, the adjustment factors  $m$  and the standard Z-R relation, respectively.

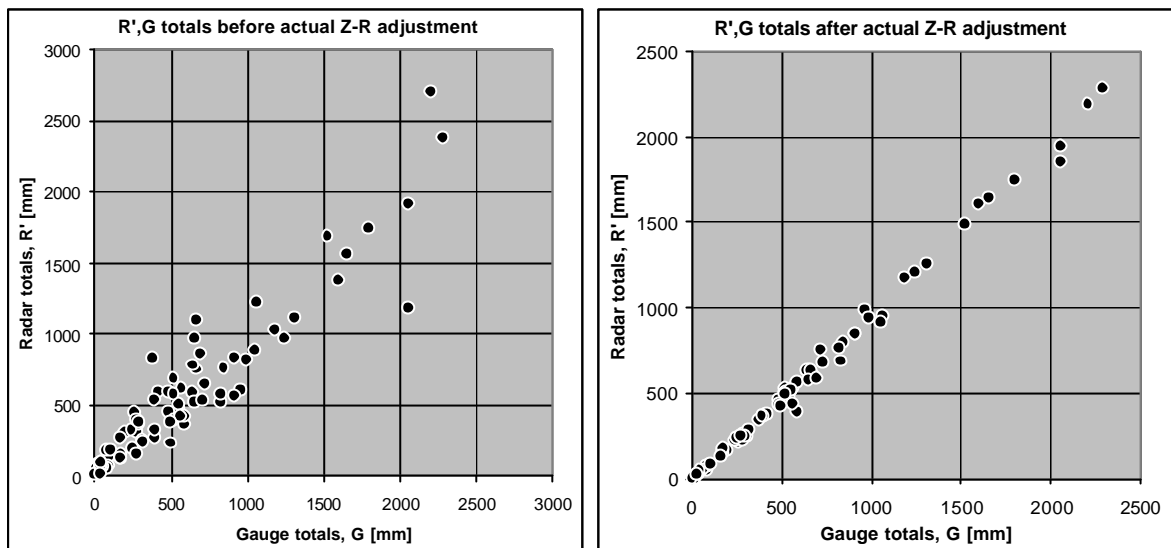


Figure 2.13. The overall results of the actual Z-R adjustment for 1998 and 1999. The gauge and radar totals are estimated by summing up all R' and G comparisons. The average amount of rain for the whole radar area is estimated by the radar or gauge total divided by the number of raingauges. Left: rain totals before the Z-R adjustment is applied. Right: rain totals after the Z-R adjustment is applied.

Figure 2.13 shows the overall results before and after the actual Z-R relations have been applied to the radar totals. Each point represents the gauge and radar totals,  $R'$  and  $G$ , on each day, but the plot do not say anything about the daily values of the individual scatter on  $G$  and  $R'$ . It is seen, that the Z-R adjustment improves the radar estimates by reducing the under- and overestimation of the radar rainfall which is clearly seen before the adjustment is carried out, i.e. the overall bias is reduced. The average amount of rain at each raingauge can be estimated by dividing the radar or gauge total by the number of raingauges.

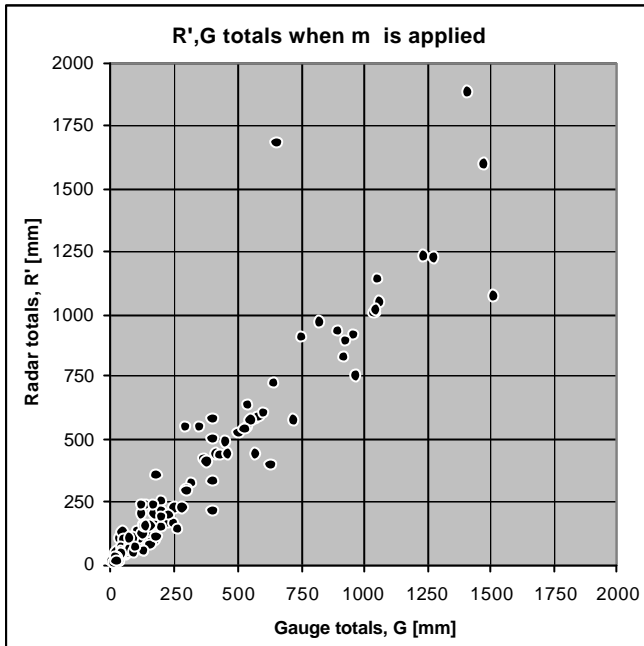


Figure 2.14. The overall results of the adjustment factor  $m$  for 1998 and 1999. The gauge and radar totals are estimated by summing up all  $R'$  and  $G$  comparisons. The average amount of rain for the whole radar area is estimated by the radar or gauge total divided by the number of raingauges.

Figure 2.14 shows the overall performance of the adjustment factor  $m$ . When  $m$  is applied, the scatter disappears but it has no meaning to show this because the method is designed at revealing adjustments for problems with the radar sensitivity as argued in the description of the method in the chapter about this.

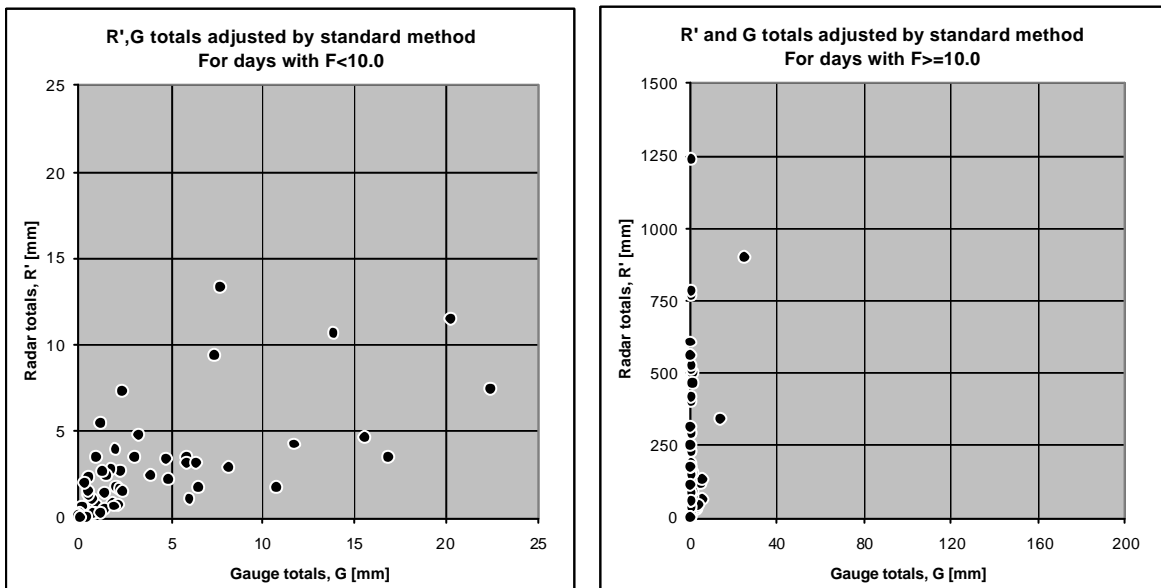


Figure 2.15. The overall results of the standard Z-R adjustment for 1998 and 1999. Left: adjustment results if  $F < 10$ . Right: adjustment results if  $F \geq 10$ . The gauge and radar totals are estimated by summing up all  $R'$  and  $G$  comparisons. The average amount of rain for the whole radar area is estimated by the radar or gauge total divided by the number of raingauges.

It is very interesting to see, what happens when the adjustment factor fails and a standard Z-R adjustment is applied (Figure 2.15). When  $F < 10$ , there has probably not been ananprop, especially when  $F$  is close to 3 or below, and on many days the radar over- or underestimates the amount of rain. If  $F = 10$ , it follows from the discussions in the chapter about ananprop identification that there may be very big problems with ananprop contamination in the radar images.

### 2.3.6 July 14<sup>th</sup>, 1998: A Cold Front

At larger ranges, the radar obviously underestimates the precipitation amount, but within 100 km range, the radar shows the precipitation pattern quite well. In the radar images from 14 Juli 1999 at 12UTC, it is seen that the precipitation echoes are becoming weaker at the larges ranges. In the overlap areas, the two radars are seeing almost the same distribution of precipitation but the rain rate is different (figure 2.16).

Up to a distance of at least 100 km, radar data can be used quantitatively, but at large ranges it can most often only be used qualitatively unless data is corrected for range related sources of error which can improve results to a certain extent. In the scatter plots in figure 2.17 is shown the R' and G samples for both radar areas, estimated for raingauge locations up to a 100 km's distance from the radar.

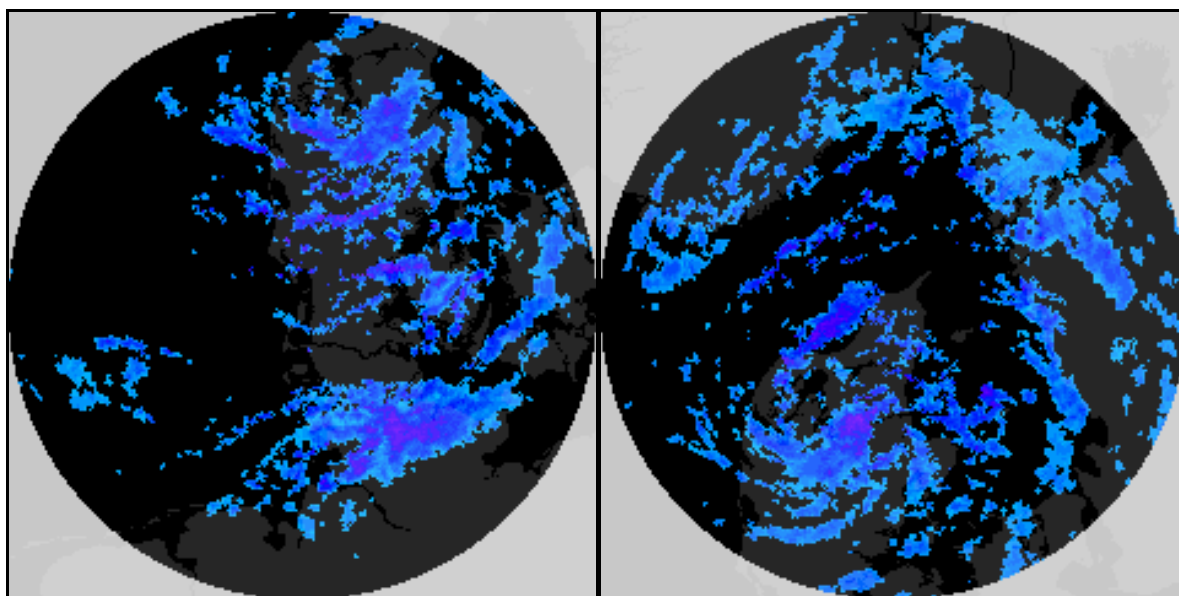


Figure 2.16. Rømø (left) and Sindal (right) images on 14 July 1998 at 12UTC. Reddish blue indicates the heaviest rain, and light blue is the weakest.

The scatter plot shows, that there is a quite large spread in the samples, but that the scatter has a structure looking like an ice cake, which is well in accordance with the multiplicative structure of the Z-R model. The representativeness problem might explain much of the large and often extreme scatter between radar measures and raingauge data (Joss, 1990), and is due to small-scale variability and gradients of precipitation, differences in the characteristics of samples from radar and raingauges.



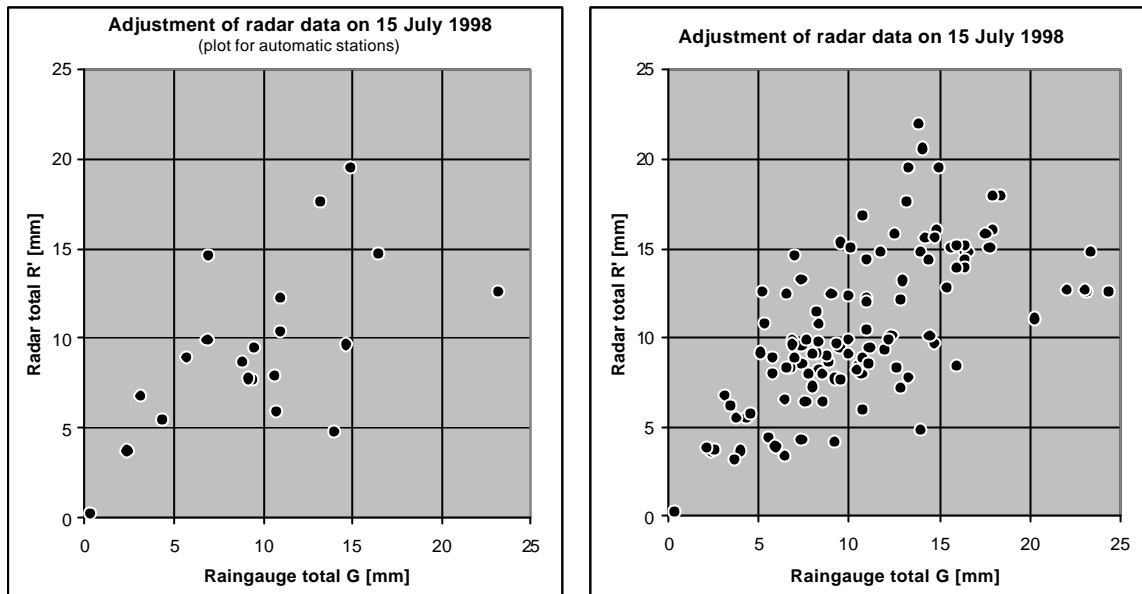


Figure 2.17. Scatter plots of individual R' and G samples on 15 July 1998. Left: R' and G samples for automatic synoptic stations is plotted. Right: R' and G samples are plotted for all comparisons. Prad=unadjusted radar samples, ZRadj=adjusted radar samples.

The radar measures the meteorological targets within a volume of air at a certain altitude above the ground surface, but the raingauge measures only a very small proportion of these particles, i.e. a pixel representing  $2 \times 2 \text{ km}^2$  is compared with a point measure. The drop size distribution may have changed until the rain hits the raingauge, and evaporation or precipitation growth may have taken place (e.g. Austin, 1987). The effect of updrafts and downdrafts can influence the accuracy of the radar and raingauge comparison (Battan, 1976), and partially and non-uniform beam filling combined with reduced visibility may lead to considerable errors at longer ranges (Joss et al., 1995).

The plot shows, that the Z-R adjustment generally results in a slight increase in the radar totals, and it has as effect that the radar do not underestimate the amount of rain. The correlation analyses resulted in  $r^2=0.79$  ( $r=0.89$ ) for the Z-R relation in the log domain, and the calculated Z-R relation is  $Z=198R^{1.48}$ . The standard error of the residuals ( $1 \times$  standard deviation) is 3.86.

### 2.3.7 June 24<sup>th</sup>, 1999: Showers

Figure 2.18 shows two illustrative examples of what the problem is about when adjusting radar images in case of showers. The precipitation pattern is scattered, but the showers were quite heavy. Some raingauge stations got more than 10 mm of rain, and one station got about 23 mm during the 24-hour period (Figure 2.19).

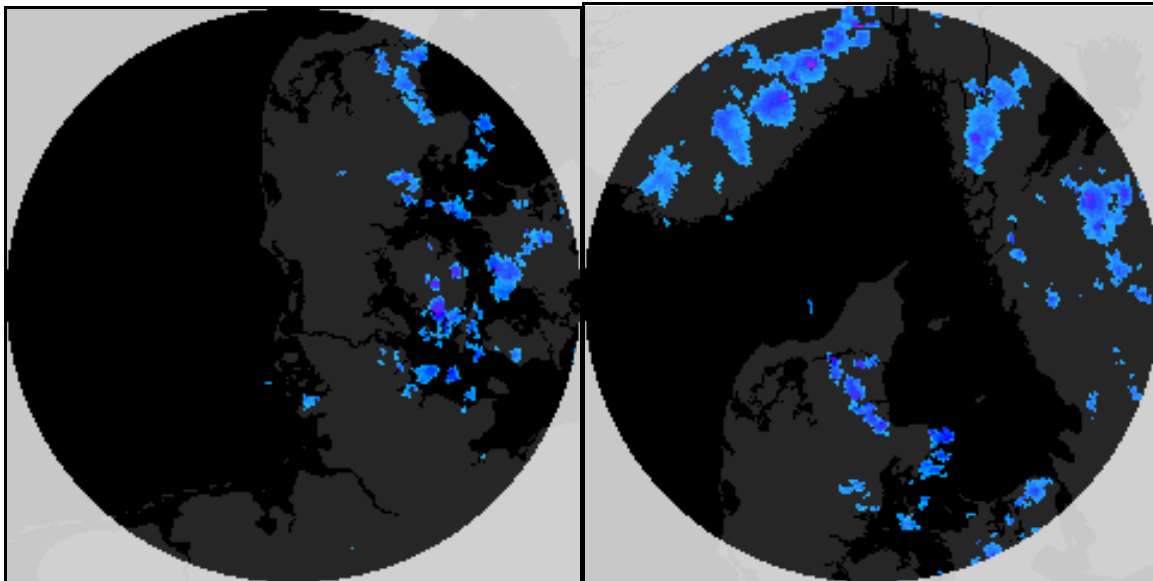


Figure 2.18. Rømø (left) and Sindal (right) radar images on June 24<sup>th</sup> 1999 at 15 UTC. Reddish blue indicates the heaviest rain, and light blue is the weakest.

In figure 2.19 is seen, that there is a large scatter in the G and R' comparison, as expected, because it is a situation with showers where the radar sample may not represent the situation at the raingauge station, or the opposite. The correlation analyses resulted in  $r^2=0.89$  ( $r=0.94$ ) for the Z-R relation in the log domain, and the calculated Z-R relation is  $Z=222R^{1.48}$ . The standard error of the residuals ( $1 \times$  standard deviation) is 3.13.

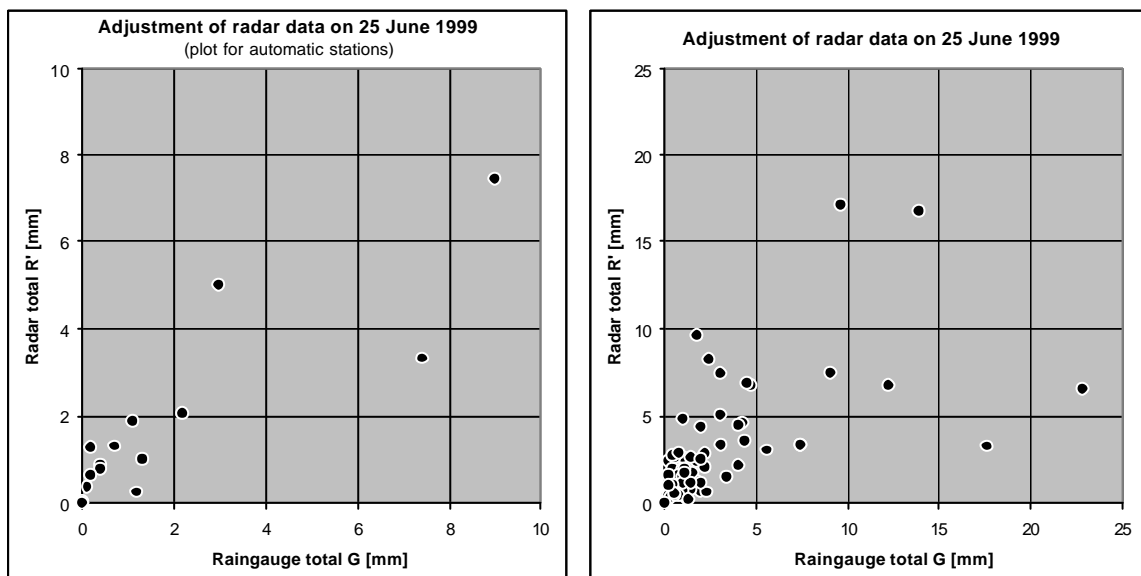


Figure 2.19. Scatter plots of individual R' and G samples on 25 June 1999. Left: R' and G samples for automatic synoptic stations is plotted. Right: R' and G samples are plotted for all comparisons. Prad=unadjusted radar samples, ZRadj=adjusted radar samples.

During showers, there are often large horizontal variations in the rain rate, and there is an increased risk that the radar over- and underestimates the total amount of rain. There seems to be a marked difference between the GR comparison for automatic synop stations, and all stations including

manual raingauge stations. The result for synop stations only is better than when all stations are included. The reason may be that the raingauge at manual stations is not emptied at exactly the same time. There is also the risk that some of the manual stations represent accumulation over more than one day, and that the value on a specific day is an estimated one.

### 2.3.8 August 5<sup>th</sup>, 1999: Anaprop

During anaprop, the refraction of the radar beam causes it to be bended downwards more than the curvature of Earth, and it hits targets on the ground randomly at nearly all ranges. The result is artificial radar precipitation amounts unless correction for this effect is applied. Methods exist for dampening or removal of anaprop, but this requires careful filtering of the images, especially because anaprop and precipitation may appear in the same image.

Figure 2.20 shows severe anaprop in a Sindal image on August 5<sup>th</sup> 1999 at 6 UTC. The effect of the terrain shows up as distinct echoes due to the coastal areas of Southern Norway, Sweden, Zealand and Jutland. The scatter plot shows that something spurious is really going on. The value of F was 1479.9, which indicates heavy anaprop according to the definition of F.

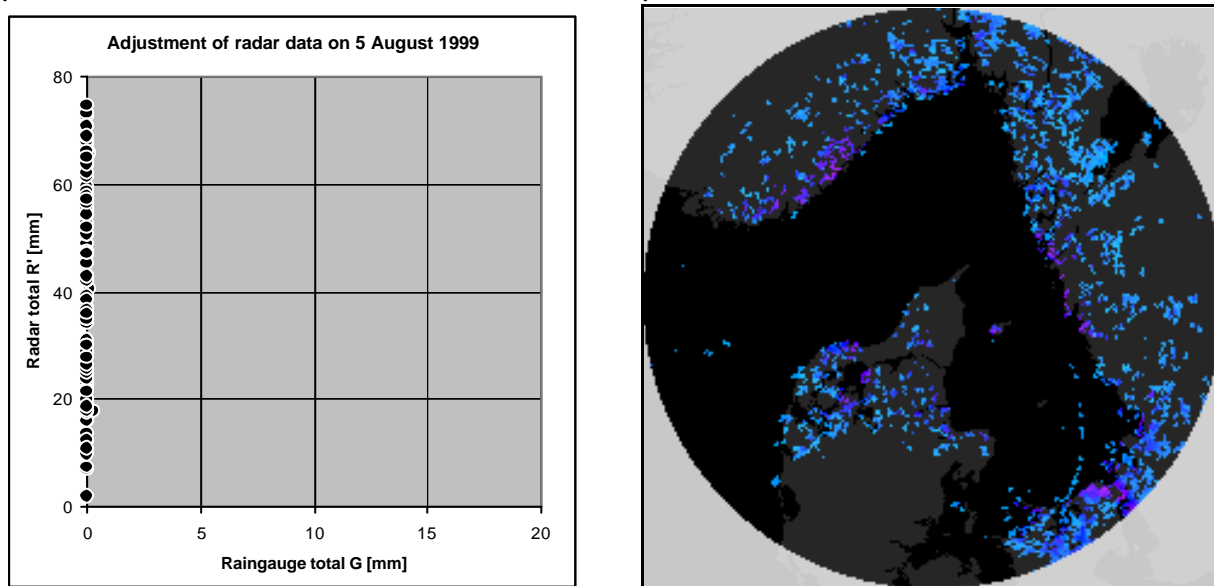


Figure 2.20. Left: scatter plots of individual R' and G samples on 5 August 1999. The R' and G samples are plotted for all comparisons. Right: an anaprop contaminated radar image (Sindal radar image) on 5 August 1999 at 6 UTC. Reddish blue indicates the heaviest rain, and light blue is the weakest.

### 2.3.9 August 19<sup>th</sup>, 1999: Heavy Precipitation

The area got widespread and heavy convective precipitation at places. As shown by the radar images in figure 2.21, the precipitation was at the same time widespread at some places and isolated at others in form of smaller heavy showers.

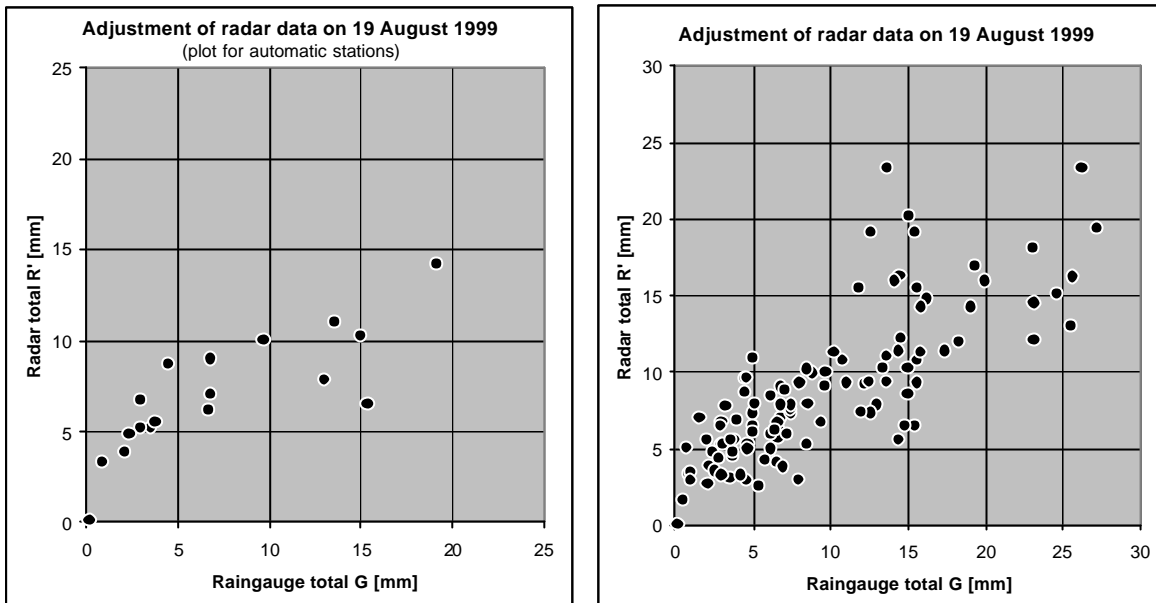


Figure 2.21. Scatter plots of individual R' and G samples on 19 August 1999. Left: R' and G samples for automatic synoptic stations is plotted. Right: R' and G samples are plotted for all comparisons.

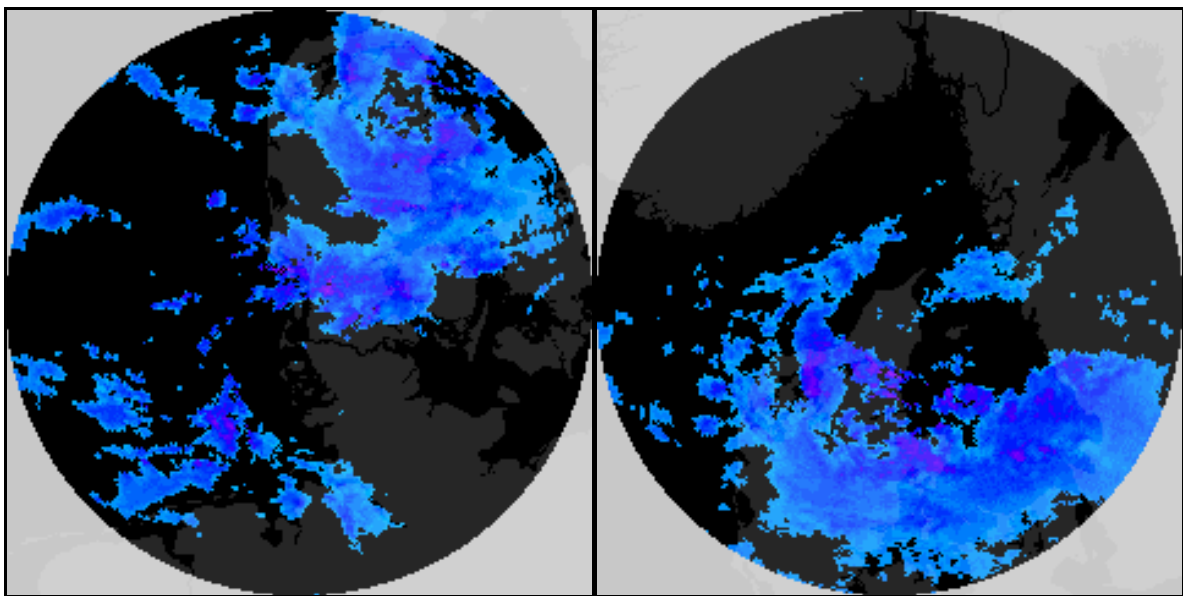


Figure 2.22. Radar images from Rømø (left) and Sindal (right) on August 19<sup>th</sup> 1999 at 6 UTC. Dark blue indicates the heaviest rain, yellow and grey is the weakest. Reddish blue indicates the heaviest rain, and light blue is the weakest.

The scatter plot in figure 2.21 shows the expected scatter between radar and raingauges, and the spread around the identity line looks like a cone structure pointing towards the intersection between the x- and y-axis. The correlation analyses resulted in  $r^2=0.80$  ( $r=0.985$ ) for the Z-R relation in the log domain, and the calculated Z-R relation is  $Z=475R^{1.31}$ . The standard error of the residuals ( $1 \times$  standard deviation) is 6.00.

Due to the spatial differences in the precipitation pattern, there are probably rather large

differences in the drop size distribution in the rain area. The performance of raingauge adjustment depends on the precipitation type (e.g. Koistinen and Puhakka, 1984, Jacquet, Andrieu and Denoeux, 1987, Austin, 1987), and the drop size distribution governing the reflectivity factor may show considerable spatial and temporal variations, even within the same rain area (Stout and Mueller, 1968). The scatter plot suggest the possibility of this, because it seems that the radar is overestimating for small amounts of rain, but underestimating for large totals at the raingauge stations.

Moreover, C-band radars are generally sufficient for monitoring moderate precipitation events, but for monitoring of heavy storms there would probably be no energy left in the radar beam for detection of hydrometeors from the far side of the storm. This effect may also have been affecting the result of the radar and gauge comparison. For example, in the Sindal image in figure 2.22 the southern edge of the rain area appears rather ambiguous, but the same edge found in the Rømø image is very distinct and with much higher echo intensities.

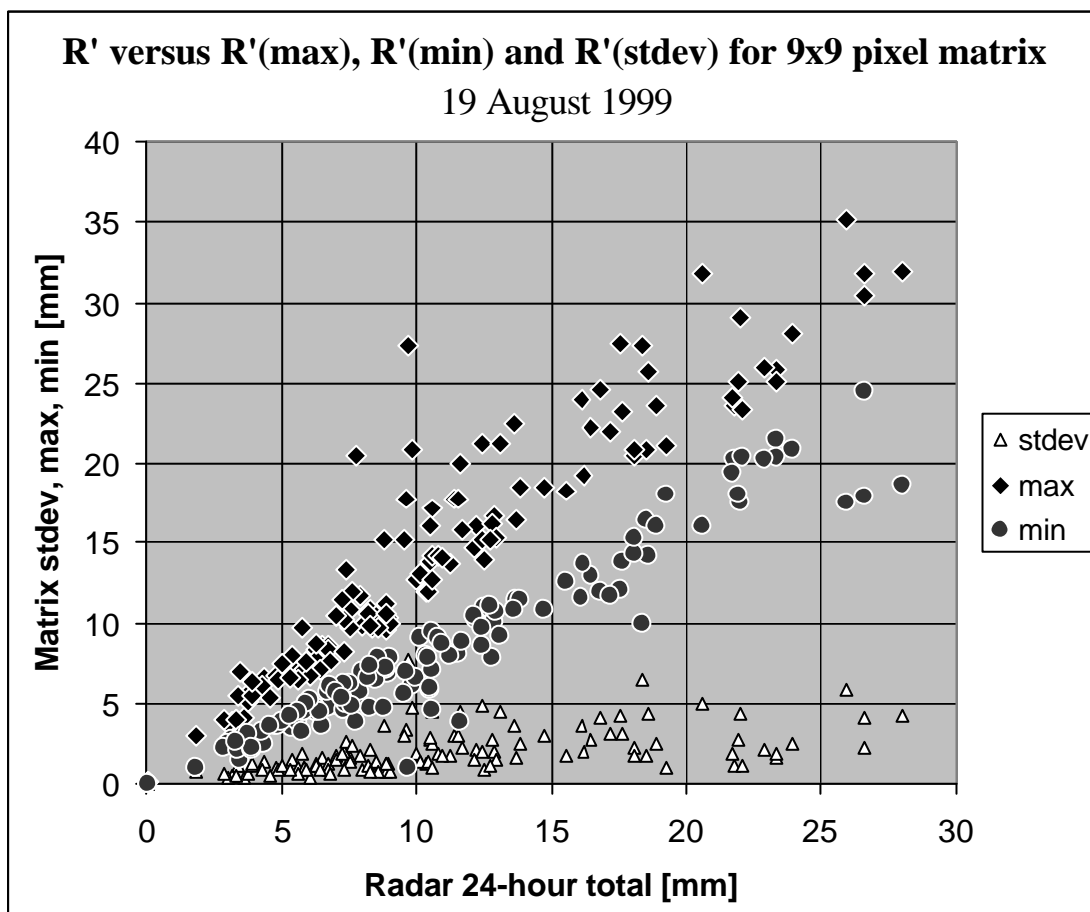


Figure 2.23. Illustration of the small-scale spatial variation in radar precipitation amount within a 9x9 pixel matrix, for which is shown the standard deviation (stdev), maximum value of R' (max) and minimum value of R' (min).

To illustrate the problem of small-scale spatial variations in the radar amount of precipitation, Figure 2.23 shows a scatter plot of the standard deviation, maximum and minimum value of the radar total for a 9x9 pixel matrix situation around the raingauge location. The spatial dimension of a

pixel is  $2 \times 2 \text{ km}^2$ . The spatial variations can be quite extensive, especially for large values of the radar total in this specific weather situation. For example, the pixel with the largest value of  $R' = 28.0 \text{ mm}$ , had variations of  $R'$  between 18.7 and 32.0 mm in the neighbour pixels. Therefore, the raingauge adjustment could be improved if corrections for this effect is incorporated, e.g. by resampling of the images.

These effects may argue for implementation of improvements of the adjustment scheme in order to take the spatial variability of precipitation systems into account.

### **2.3.10 Conclusions and outlook**

The analyses of anaprop lead to the conclusion, that estimation of F and using a threshold value  $z=3$  is a good method for identification of 24-hour image sequences probably contaminated by anaprop. In few cases with a high value of F isolated showers may be present, but the amount of precipitation should be limited in most cases. It is better to exclude anaprop days from the calculation of AMIS fields than using spurious looking radar totals, even though small rain areas may have been present.

When anaprop and precipitation is present in the same image or during the accumulation period of the raingauges, other anaprop identification methods than the one supposed should be developed. For example, satellite information could help the identification of no-rain areas, or analyses of the reflectivity distribution in radar images and analyses of the Polar data volume of the radar could enter a correction method for reduction of the anaprop problem.

C-band radars are generally sufficient in monitoring moderate precipitation events, but in heavy rain storms there would probably be no energy left in the radar beam for detection of hydrometeors from the far side of the storm. On average, reflectivity will decrease with range due to the increasing height of the radar beam. According to Kitchen and Jackson (1993) the underestimation of rainfall accumulations at longer ranges ( $>100 \text{ km}$ ) is mainly caused by a steep decline in probability of detection and not so much by underestimation of the precipitation rate in each image. The subsequent rainfall accumulation might be subject to significant underestimation, and range adjustments should be applied to improve the radar performance at long range.

Following Kitchen (1995), the poor understanding of the uncertainty in gauge adjustment does not support a complex method. A wide range of Z-R relationships have been derived which generally is ascribed to the natural variability of drop-size distributions. This variability introduces one of many errors and not the most severe at that.

The adjustment approach in this study focuses on correction of systematic errors on radar data in the whole image. It does not assign real-time, or near real-time raingauge adjustments which may vary over the radar image as demonstrated by Lord and Young (1994). Local adjustments based on a small number of Z-R comparisons may cause the adjustment surface to vary in an unrealistic manner because of a too low number of degrees of freedom, and the effect of not representative

samples would have a too big effect on the adjustment. The adjustment system could be improved by taking into account the variability of a precipitation system in a better way. On the other hand, the adjustment system may have difficulties in deriving reliable model parameters in some events. In homogeneous rain areas, the adjustment is quite stable, but in case of showers, or different precipitation types in the same radar image, it may be difficult to derive confident parameter values. Isolated showers may pass the raingauge network and not monitored, and the image retains standard calibration. If the precipitation types in the radar image are recognized and appropriate Z-R adjustments are applied, the adjustment results could be better.

The effect of not representative samples can be reduced by using many Z-R values in the same rainfall system (Austin, 1987), and the scatter between the two measures can be reduced by increasing the integration period. On the other hand, many samples do not remove the scatter in the individual measurements (Zawadski, 1984).

The bright-band effect can have a substantial effect on the precipitation estimates in the beginning of the growth season, and a method for correction of this effect could gain improvements of the radar rain estimates.

Finally, the radar integration should take into account the velocity of a precipitation area. If the integration of radar data is not treated correctly, the so-called "fishbone" effect might appear in the integrated radar image (Bellon, Fabry and Austin, 1991). From a hypothetical experiment, they found that errors caused by an improper accumulation procedure could be larger than those caused by inaccurate Z-R relations.

To sum up possibilities for improvements of the grid estimates:

- Apply improved methods for anaprop removal.
- Implement improved estimation of radar totals.
- Implement a bright-band correction method.
- Implement correction for vertical reflectivity profile variations.
- Take into account the velocity of precipitation systems.

## **3. Verification**

### **3.1 Data**

The objective verification has been done for the two growing seasons separately, i. e. for April 1 to September 30 1998 and for April 1 to September 30 1999. For the radar derived 24 hour accumulated precipitation and all the observation based 24 hour accumulated precipitation fields, the field data has been further stratified according to month. Result are calculated for each month for both years.

The raw radar data are subject to the same restrictions as in phase I. Statistics for the amount radar data is given in the report "Evaluation of the AMIS Gridded Observations and Radar derived 24-hour Accumulated Precipitation by Comparison with Climate – Grid Denmark Gridded Observations" phase I.

### **3.2 Verification Methods**

All data fields are verified against the Climate Grid - Denmark. For each matched grid point the mean error (ME), the mean absolute error (MAE) and the root mean square error (RMSE) is calculated on monthly basis.

Contingency tables with categories 0-0.05, 0.05-2, 2-6, 6-10 and 10-100 mm precipitation/24hr for all fields has been constructed. The contingency tables for the growing seasons are presented below. The contingency tables for each month are placed in appendices C to J. Based on the contingency tables the hit rate (HR) and Hansson Kuipers skill index (HKSI) are calculated for each grid point for every month in the growing seasons.

The maximum, the mean and the minimum value of the ME, MAE and HR values of all the grid points covering Jutland are presented in a graphical form for each month in the growing seasons. Tables of all the verification parameters are placed in appendix B.

## **3.3 Results: Increasing Number of Stations in the Interpolation**

### **3.3.1 1998**

Table 3.1 shows for the whole growing seasons 1998 the contingency tables for the four precipitation fields with the 25 observations in the interpolation at the top and then increasing the number of observations downwards. The corresponding monthly contingency tables are placed in the appendices.



25 KLIMA		0	0.05	2	6	10	mm nedbør
AMIS		0.05	2	6	10	100	
0	0.05	18331	1764	53	12	5	
0.05	2	8991	15253	2552	122	16	
2	6	116	2403	8000	1143	208	
6	10	14	150	1420	2303	777	
10	100	0	23	181	762	3067	

mm nedbør

62 KLIMA		0	0.05	2	6	10	mm nedbør
AMIS		0.05	2	6	10	100	
0	0.05	21483	1711	23	1	0	
0.05	2	5950	15763	1842	61	9	
2	6	30	2050	9084	1026	107	
6	10	0	65	1157	2605	654	
10	100	0	5	99	650	3303	

mm nedbør

87 KLIMA		0	0.05	2	6	10	mm nedbør
AMIS		0.05	2	6	10	100	
0	0.05	22437	1761	17	0	0	
0.05	2	5006	16031	1725	45	8	
2	6	23	1760	9375	964	96	
6	10	0	44	1010	2729	586	
10	100	0	1	80	605	3383	

mm nedbør

126 KLIMA		0	0.05	2	6	10	mm nedbør
AMIS		0.05	2	6	10	100	
0	0.05	22800	1686	11	0	0	
0.05	2	4652	16229	1698	37	7	
2	6	15	1648	9472	956	80	
6	10	0	33	955	2766	565	
10	100	0	2	68	583	3421	

mm nedbør

Table 3.1 Contingency table for April 1<sup>st</sup> 1998 to September 30<sup>th</sup> 1998.

The values in the off-diagonal elements representing either over- or underestimation of the precipitation amount compared to Climate-Grid are quit large, when only 25 observations are used in the interpolation. However already with 62 observations used, these values has dropped significantly. Increasing the number of observations further to 87 and 126 continues to reduce the value of the off-diagonal elements but at a much slower rate. The values in the diagonal elements representing the correct categories of cause increase correspondingly especially for small amounts

of precipitation. 87 observations seems to be close to an optimum amount of observations judged from contingency tables.

Figure 3.1 show curves for the ME (a), MAE (b) and HR (c) verification measures for each month in the growing season 1998. The blue curves is calculated with 25 observations, the red curve with 62 observations, the yellow curve with 87 observations and the green curve with 126 observations in the interpolation. Finally the operational AMIS is represented by a black curve. For each verification measure three sets of diagrams are shown one for the minimum value, one for the mean value and one for the maximum value all taken over all grid points in the month.

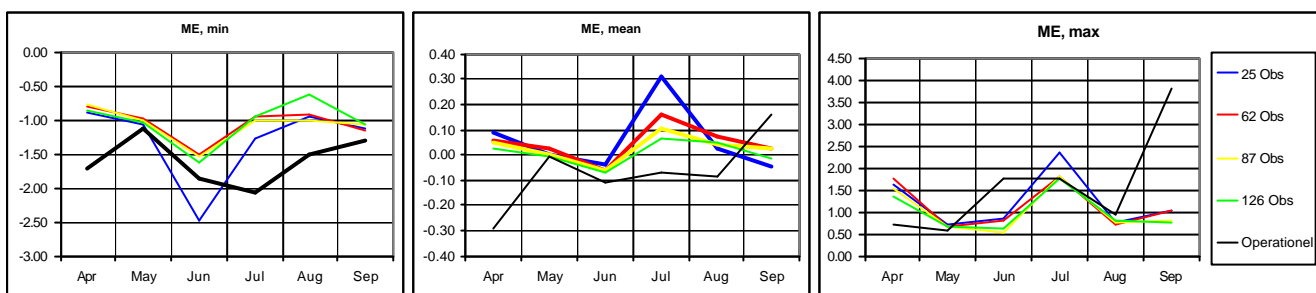


Figure 3.1a. ME. Minimum, mean and maximum.

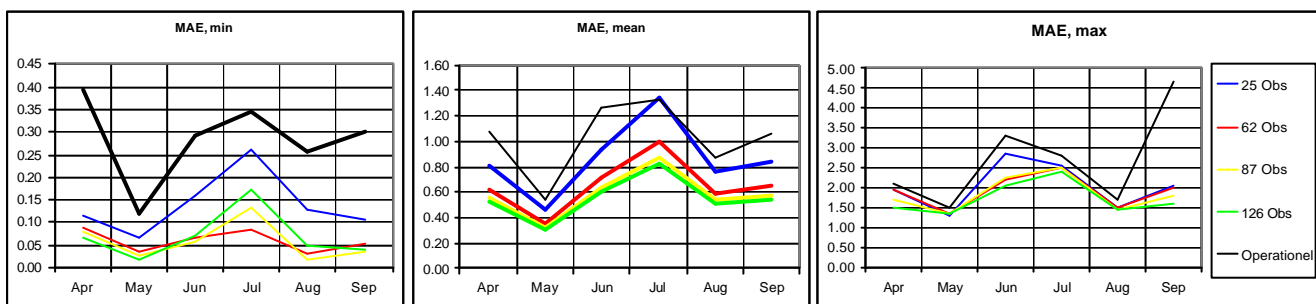


Figure 3.1b. MAE. Minimum, mean and maximum.

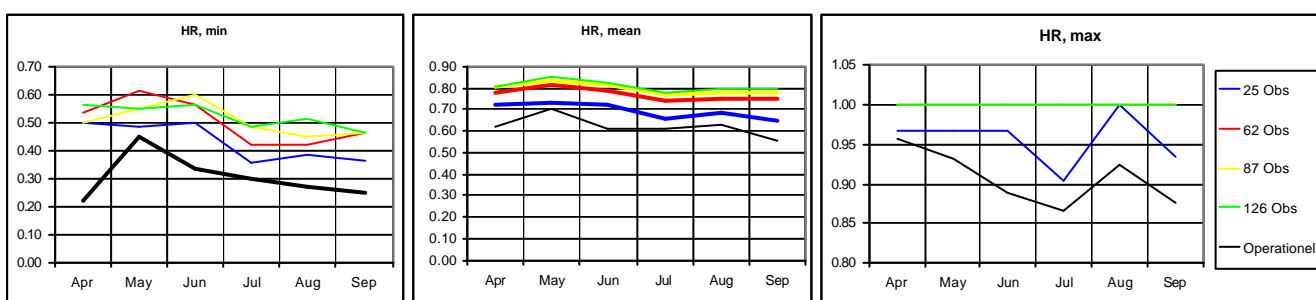


Figure 3.1c. HR. Minimum, mean and maximum.

The minimum ME decreases as the number of observations in the interpolation increases and with 87 and 126 observations the minimum ME is closer to zero than the operational AMIS at that time. The mean ME has become positive for some of the months in the growing season especially July. The mean ME has been improved significantly though with only small improvements going to 87 and 126 observations in the interpolation. The large maximum ME in September in the operational AMIS is reduced from more than 3.5 to around 1. The large maximum ME in the

operational AMIS was due to a reported precipitation amount of 14 mm/12hr September 9<sup>th</sup> at 18:00 UTC at station Bågø (06111), see phase I report. This station was not used in the 25 station sample explaining why the maximum ME even in this case is small. However the Bågø station is included in the samples with more observations and the wrong observation is thus suppressed by the larger amount of the other more correct observations.

The MAE is decreasing for both minimum, mean and maximum values as the number of observations in the interpolation is increasing, with the minimum value having the largest decrease and maximum value the smallest decrease, except again in September, where Bågø observation gives a large maximum MAE in the operational AMIS. All together a significant improvement again with no significant difference between 87 and 126 observations in the interpolation.

The HR is increasing for both minimum, mean and maximum values as the number of observations in the interpolation is increasing, with the minimum value having the largest increase and maximum value the smallest increase but with maximum hit rate around 100%

Figure 3.2 show the mean of the MAE for all months as function of the number of observations in the interpolation. The curve illustrates the already mentioned small different between 87 and 126 observations in the interpolation indicating that 87 observations is close to an optimal number of observations. Adding further observations will not improve the results significantly.

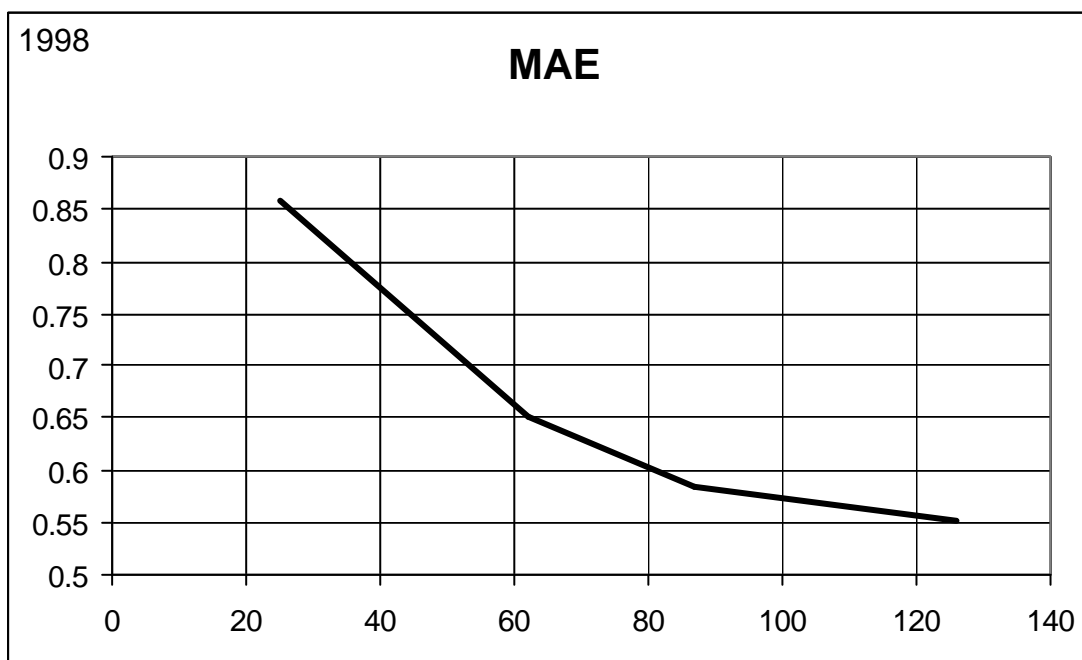


Figure 3.2 MAE absolute error as function of the number of observations used in the interpolation.

### 3.3.2 1999

Table 3.2 shows for the whole growing seasons 1999 the contingency tables for the four precipitation fields with the 25 observations in the interpolation at the top and then increasing the number of observations downwards. The corresponding monthly contingency tables are placed in the appendices.

25 KLIMA		0	0.05	2	6	10	mm
AMIS		0.05	2	6	10	100	nedbør
0	0.05	25251	1111	29	9	3	
0.05	2	8266	10521	1658	100	47	
2	6	75	2046	6144	1409	297	
6	10	1	126	1490	2489	1075	
10	100	0	58	361	1173	3901	

mm nedbør

62 KLIMA		0	0.05	2	6	10	mm
AMIS		0.05	2	6	10	100	nedbør
0	0.05	28967	1115	35	9	4	
0.05	2	4623	11126	1381	79	30	
2	6	33	1557	6726	1119	165	
6	10	0	56	1329	2933	802	
10	100	0	22	209	1039	4322	

mm nedbør

87 KLIMA		0	0.05	2	6	10	mm
AMIS		0.05	2	6	10	100	nedbør
0	0.05	29794	1207	26	2	0	
0.05	2	3801	11229	1295	73	28	
2	6	21	1370	6993	1053	149	
6	10	1	50	1219	3110	794	
10	100	0	16	144	939	4352	

mm nedbør

126 KLIMA		0	0.05	2	6	10	mm
AMIS		0.05	2	6	10	100	nedbør
0	0.05	30259	1181	24	3	0	
0.05	2	3331	11335	1329	77	33	
2	6	31	1313	7050	1041	121	
6	10	1	57	1147	3153	793	
10	100	0	10	128	906	4376	

mm nedbør

Table 3.2 Contingency table for April 1<sup>st</sup> 1999 to September 30<sup>th</sup> 1999.

Also this year the values of the off-diagonal elements decrease as the number of observations in the interpolation is increased. The tendency is however not so pronounced as in the growing season 1998.

Figure 3.3 is similar to figure 3.1 showing curves for the ME, MAE and HR but here for each month in the growing season 1999. Colours and line types are similar to figure 3.1.

Also these verification measures show the same pattern as those of 1998.

The peak in the operational AMIS September 8<sup>th</sup> is due to a reported precipitation amount of 34 mm/24hr at 06:00 UTC at station Borris II (05410). This peak is being suppressed as the number of more correct observations is added in the interpolation.

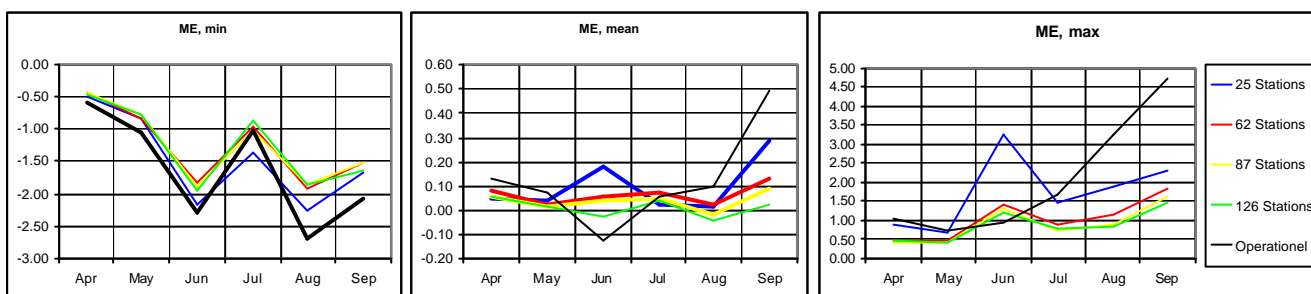


Figure 3.3a. ME. Minimum, mean and maximum.

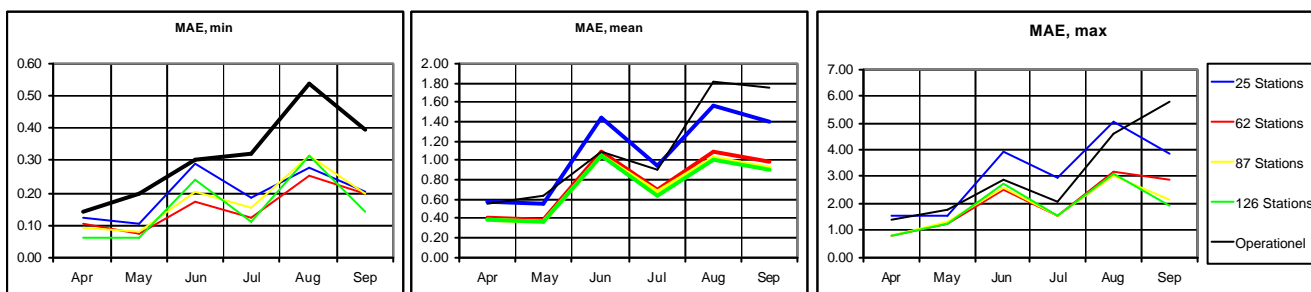


Figure 3.3b. MAE. Minimum, mean and maximum.

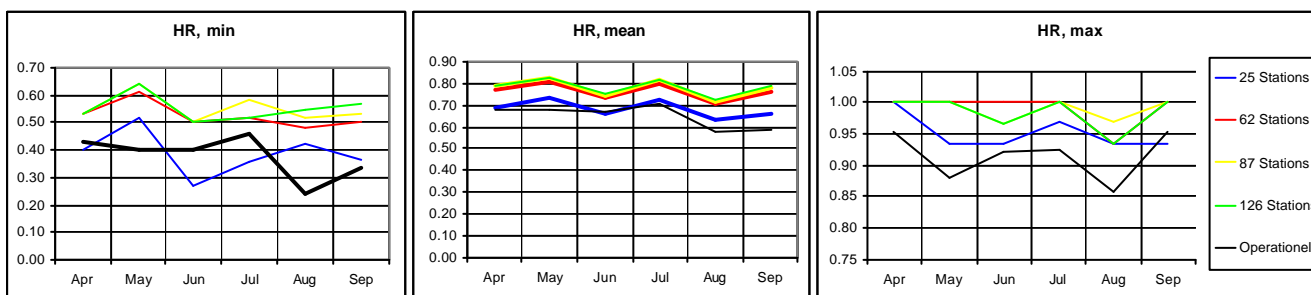


Figure 3.3c. HR. Minimum, mean and maximum.

Figure 3.4 show the mean of the MAE for all months as function of the number of observations in the interpolation for 1999 and is similar to figure 3.2 for 1998. This year 62 observations seems to be close to an optimal number of observations.

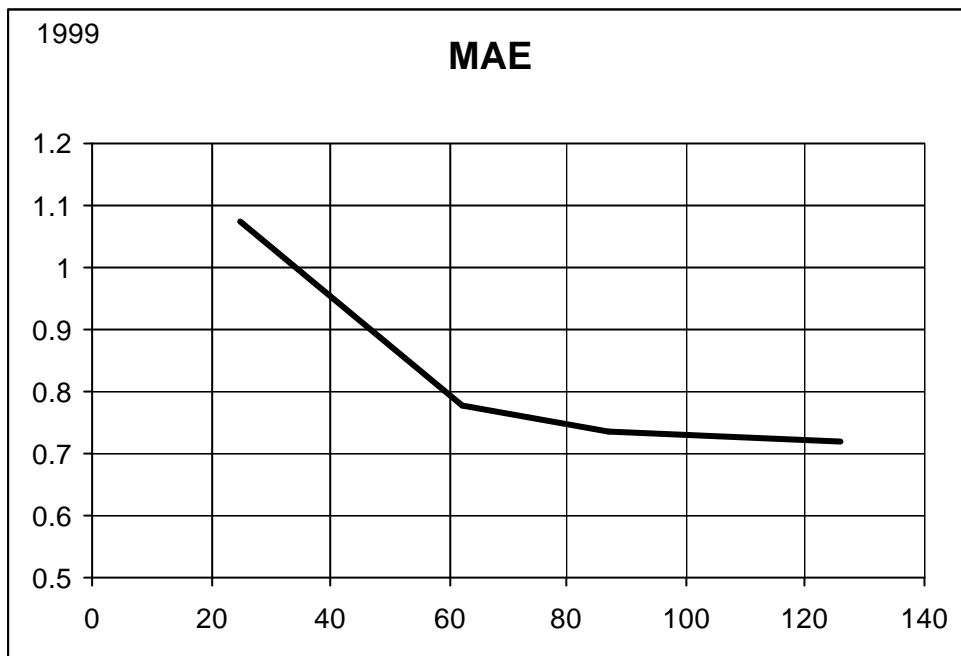


Figure 3.4 MAE absolute error as function of the number of observations used in the interpolation.

### 3.4 Results: Radar

In phase I it has been demonstrated, that the overall statistical verification measure for the radar derived 24-hour accumulated precipitation are not as good as those for the operational AMIS. The reason for this was partly due to anaprop and the use of raw uncalibrated radar data. The aim of phase II is to correct the radar data for anaprop errors and to adjust the radar derived 24-hour accumulated precipitation to get overall statistical verification measures comparable to AMIS. The results of this part of the phase II study are presented for the growing season 1999 first, because this year had 26 days with anaprop whereas 1998 had only 2, see chapter 2.3.3. The adjustment has been performed using SYNOP (automatic) observations only since the observations reported daily on phone had a relative poor correspondence with the radar derived precipitation.

#### 3.4.1 1999

Figure 3.5 show curves for the ME (a), MAE (b) and HR (c) verification measures for each month in the growing season 1999. The blue curve is the result from phase I. The red curve shows the verifications measures after anaprop days has been put equal to 0. In 1999 as mention the number of days with anaprop is 26, see chapter 2.3.3. The green curve shows the verifications measures when the anaprop days has been put equal to 0 and the radar derived precipitation has been calibrated using the method described in chapter 2.3.4. The yellow curve shows the verifications

measures after adjustment of the radar derived precipitation and elimination of days with a large difference in the precipitation sum. This is done by removing day with  $F > 10$  the ratio of radar derived precipitation sum to observed precipitation sum (see chapter 2.3.3). The result is that some days will be eliminated even if it is not a day with anaprop but just a bad day. The method will however also remove days with anaprop so a separate anaprop procedure is unnecessary.

Finally the operational AMIS is represented by a black curve. For each verification measure three sets of diagrams are shown one for the minimum value, one for the mean value and one for the maximum value all taken over all grid points in the month.

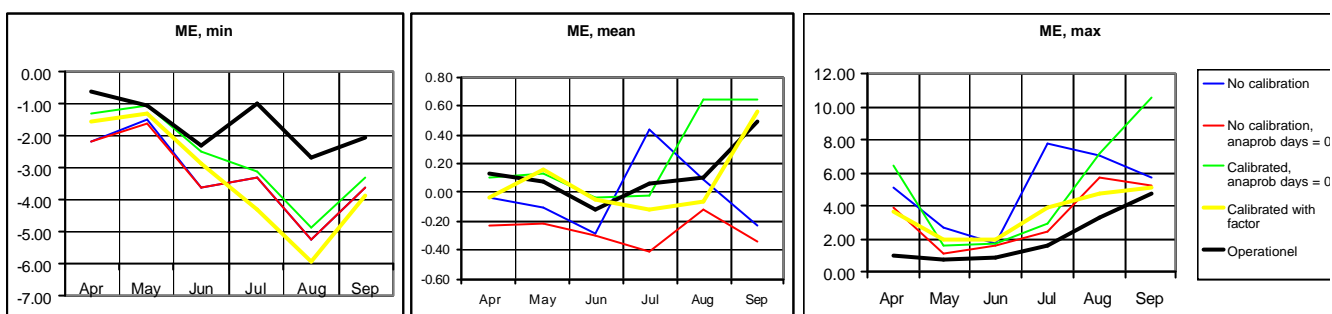


Figure 3.5a. ME. Minimum, mean and maximum.

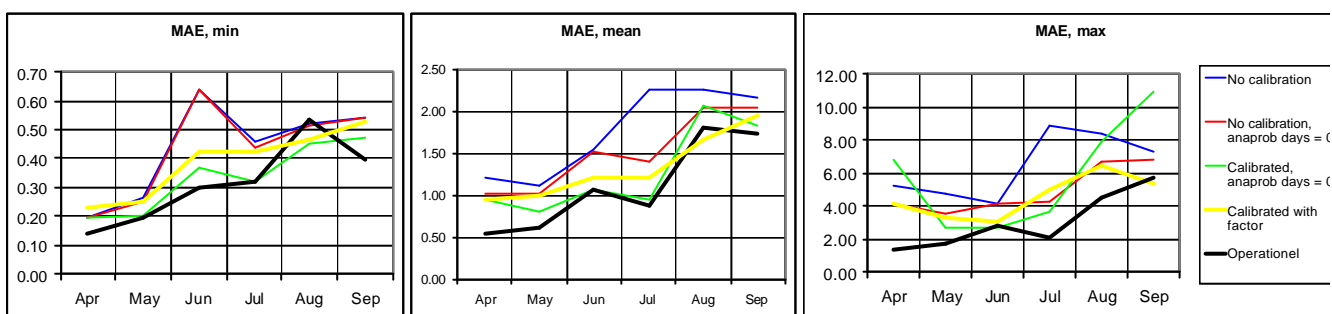


Figure 3.5b. MAE. Minimum, mean and maximum.

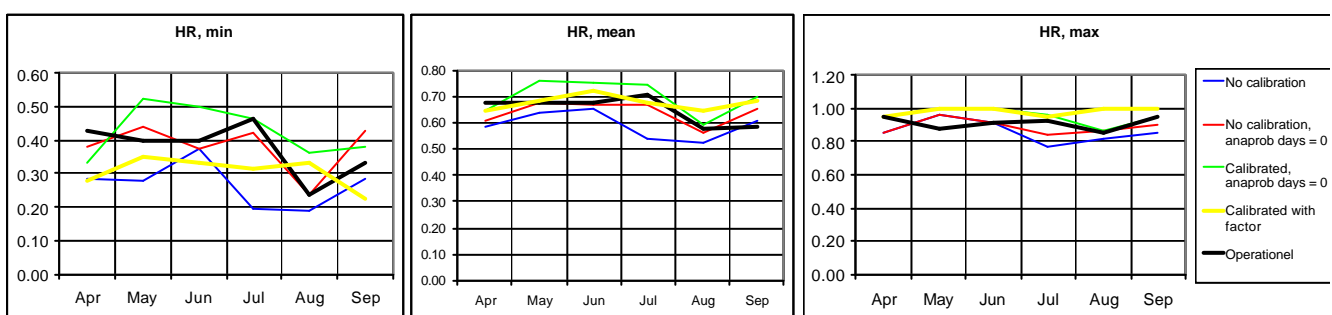


Figure 3.5c. HR. Minimum, mean and maximum.

The minimum ME values are not changing much for any of the four radar derived precipitation fields. This is more or less expected since anaprop correction and calibration will have the largest impact on the largest differences from the true (Climate-Grid Denmark)

The mean ME is somewhat better with anaprop correction than without and even more when adjustment is performed. The method with adjusted radar derived precipitation and elimination of bad days has improved the mean ME so that it is comparable with the operational AMIS. This is also the situation for the maximum ME, where the method with adjusted radar derived precipitation and elimination of bad days reduces the maximum ME of 10 reached for the anaprop correction and adjustment (green curve) to about 4, which is just above the operational AMIS.

The minimum MAE for the anaprop corrected field is no better than without the correction. Adjusted and anaprop corrected field (green curve) and the field from the method with adjusted radar derived precipitation and elimination of bad days are both closer to the operational AMIS than the unadjusted fields especially in June, with the adjusted and anaprop corrected field being the best. However the method with adjusted radar derived precipitation and elimination of bad days though is still comparable to the operational AMIS.

The anaprop corrected field reduces the mean MAE compared to the original field, but again here the adjusted and anaprop corrected field and the field from the method with adjusted radar derived precipitation and elimination of bad days are both comparable to the operational AMIS, with the adjusted and anaprop corrected field being the best.

The same pattern is seen for maximum MAE except here the field from the method with adjusted radar derived precipitation and elimination of bad days is much better than the adjusted and anaprop corrected field in April and September. This is the reason why the method with adjusted radar derived precipitation and elimination of bad days was introduced. This method eliminates some days in April and September, which has precipitation sum very different from the SYNOP observations and these days therefore, as seen, verify very bad.

For the minimum HR the anaprop corrected field is very close the operational field. The adjusted and anaprop corrected field and the field from the method with adjusted radar derived precipitation and elimination of bad days are not that close to the operational AMIS, but still somewhat better than the original field.

For the mean and maximum HR the adjusted and anaprop corrected field and the field from the method with adjusted radar derived precipitation and elimination of bad days both has a higher HR than the operational AMIS, except in April and July for the mean where the field from the method with adjusted radar derived precipitation and elimination of bad days is slightly smaller than the operational AMIS.

### **3.4.2 1998**

Figure 3.6 is similar to figure 3.5 curves for the ME (a), MAE (b) and HR (c) verification measures for each month, but for the growing season 1998. As mentioned before only 2 days had anaprop detected, thus it has no meaning showing the red curves representing an anaprop corrected field only (red curves in figure 3.5).



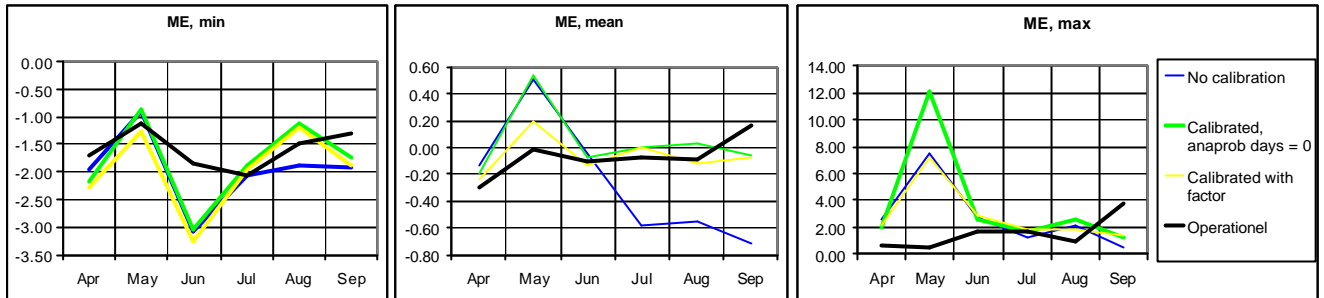


Figure 3.5a. ME. Minimum, mean and maximum.

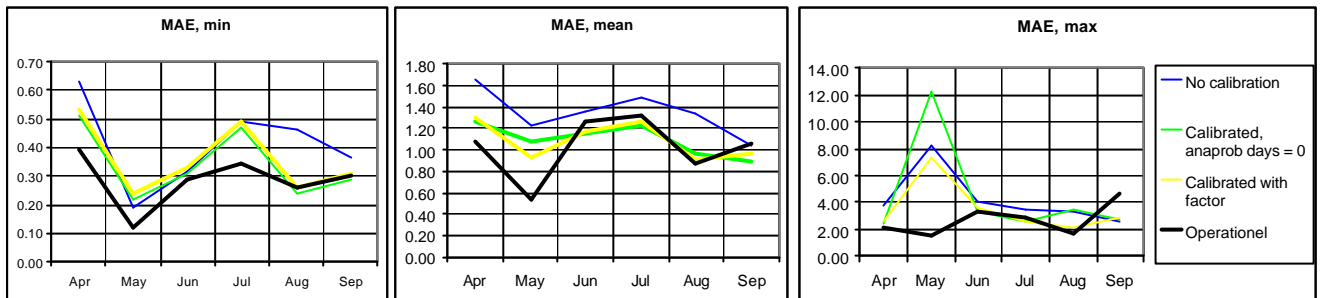


Figure 3.5b. MAE. Minimum, mean and maximum.

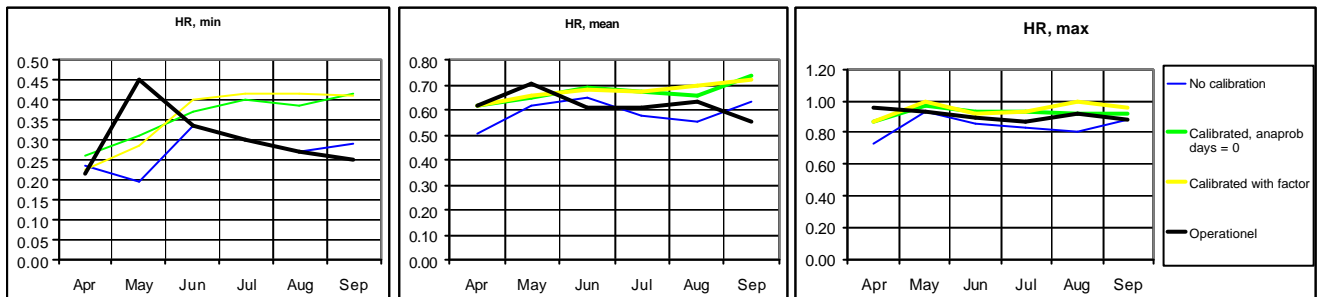


Figure 3.5c. HR. Minimum, mean and maximum.

Generally the improvements for the growing season 1998 are not as significant as they were in the growing season 1999. This is partly due to the small number of anaprob days in 1998, but also a yearly variance in the performance. On the other hand are the performance in 1998 comparable or sometimes better than in 1999, which then is difficult to improve further. However 1998 show a relative bad verification in May.

The minimum ME has not changed much from the original field. The mean and maximum ME are comparable with the operational AMIS except in May. This is due to some days with very large radar derived precipitation at a few grid points which is not found in the climate-grid Denmark. They result in a large ME value at these grid points which gives a large maximum ME and some influence on the average ME. If these grid points are removed the maximum and mean ME in May would be smaller. However it should be remembered, that Climate-Grid Denmark is not the exact true precipitation.

The minimum MAE is improved especially in August and September. The mean MAE is rather constant and better than 1999 and comparable with the operational AMIS except again in May. The same is the situation for the maximum MAE.

All hit rates are better than the operational AMIS again except in May for the minimum and mean HR, though not very much for the mean HR.

## 4. Conclusions

Increasing the number of observations in the interpolation will improve the resolution of fine structure of the precipitation pattern. This was clearly demonstrated during the case studies. These also indicated that only small improvements result from increasing the number of observations in the interpolation beyond 90. This conclusion was further supported from the overall statistical verification measures. The reduction of MAE is large going from 25 observations to 87 observations used in the interpolation, whereas only minor improvements result from further up to 126 observations, chapter 3.3. Thus 90-100 observations for Jutland seems to be a kind of optimal number of observations. This corresponds to a mean distance between observing stations of about 20 km.

The second aim of this project was to enhance the performance of radar derived precipitation so the overall statistical verification measures would be comparable to the operational AMIS values. It has been shown in chapter 3.4 that this could best be done by first using the adjustment procedure outlined in chapter 2.3.4 and then exclude days with large ratios of radar derived precipitation sums to observational precipitation sums for the whole area. Then both days with anaprop and days when the radar performs badly are excluded. The separate anaprop analysis outlined in chapter 2.3.3 is then not necessary.

Using these techniques the overall statistical measures become comparable to the operational AMIS. It should however be mentioned that one has to rely on other data sources the days the derived precipitation fields are excluded.

Some further possibilities for improving the radar derived precipitation are outlined in chapter 2.3.10

## 5. References

Austin, P. M. (1987): *Relation between measured Radar Reflectivity and Surface Rainfall*. Mon. Wea. Rev., vol. 115, p. 1053-1070.

Battan, L. J. (1973): *Radarobservation of the atmosphere*. The University of Chicago Press, Chicago, p. 1-113 and p. 324.

Battan, L. J. (1976): *Vertical air motions and the Z-R relation*. J. Appl. Meteor., vol. 14, p. 98-108.

Bellon, A., F. Fabry and G. L. Austin (1991): *Errors due to space/time sampling strategies in high resolution radar data used in hydrology*. 25th International Conference on Radar Meteorology, June 24-28, 1991, Paris, France, Am. Met. Soc., p. 840-843.

Collier, C. G. (1987): *Accuracy of Real-time Radar Measurements*. In Weather Radar and Flood Forecasting, ed. by V. Collinge and C. Kirby, Chichester 1987, p. 71-96.

Collier, C. G. (1989). *Applications of weather radar systems*. Ellis Horwood, pp 294

Joss, J. and A. Waldvogel (1987): *Precipitation measurements and hydrology*. 40. ann. Conf. on Radar Meteorology.

Joss, J., G. Galli, G. D. Bruna (1995): *Seven years of (dis-)agreement between radar, rain gauges and river flow: possible improvements?* Prepared for the 27th International Conference on Radar Meteorology 9-13 October 1995 in Vail, Colorado.

Jacquet, G., H. Andrieu and T. Denoeux (1987): *About radar rainfall measurements*. AIRH - 22nd congress - IAHR and 4th international conference on urban storm drainage, Lausanne 1987, p. 25-30.

Joss, J. (1990): *Precipitation Measurement and Hydrology. Radar in Meteorology, Battan Memorial and 40th Anniversary Radar Meteorology Conference*, Am. Met. Soc., Boston 1990, 577-606.

Kitchen and Jackson (1993): *Weather radar performance at long range - simulated and observed*. J. Appl. Met., vol. 32, 975-85.

Kitchen, M. (1995b): *Design of a gauge adjustment step for Nimrod*. Forecasting Research Division, Working Paper No. 169, Met. Office, Bracknell, UK.

Koistinen, J. and T. Puhakka (1984): *Can we calibrate radar by raingauges*. 22nd Conference On Radar Meteorology, 10-13 Sept. 1984, Zurich, Switzerland. Publ. Am. Met. Soc., 263-267.

Kreuls, R. K. (1991): *On-line calibration in HERP*. Hydrological Application of Weather Radar, ed. I. D. Cluckie and C. G. Collier, New York, 1991, 56-64.

Lord, M. E., and P. C. Young (1994): *An Improved Adaptive Calibration Technique for Weather Radar*. R & D Note 347. CRES, Lancaster University, 27 p.

Marshall, J. S. and W. McK. Palmer (1948): *The distribution of raindrops with size*. J. Meteor., vol. 5, 165-166.

Southern Water (1985): *Quantitative use of radar derived rainfall data*. Southern Water Authority, Directorate of Technical Services, Worthing, West Sussex.

Steffensen, M., Vejen, F., Hilden, A., Overgaard, S., Scharling, M., and Jüngling, H., 2001: *Evaluation of the AMIS Gridded Observations and Radar derived 24-hour Accumulated Precipitation by Comparison with Climate Grid – Denmark Gridded Observations*. DMI Technical Report 01-13, Copenhagen 2001.

Stout, G. E. and E. A. Mueller (1968): *Survey of relationships between rainfall rate and radar reflectivity in the measurements of precipitation*. J. Appl. Met., vol. 7, p. 465-474.

Zawadski, I. (1984): *Factors affecting the precision of radar measurements of rain*. 22nd Conference On Radar Meteorology, 10-13. Sept. 1984, Zürich, Switzerland. Publ. Am. Met. Soc., 251-256.

# Appendix A

## **A brief explanation of errors on weather radar data**

In the following, important sources of error on radar data will be briefly explained and discussed.

### *Clutter and anomalous beam propagation (anaprop):*

Clutter which is reflection of the radar beam from ground targets close to the radar is always more or less present in a radar image. In stable weather conditions temperature and vapour inversions may be present causing the radar beam to be refracted more than the curvature of Earth. Therefore, the beam hits ground targets at random radar ranges and artificial precipitation patterns are seen in the image (anaprop).

### *The bright-band effect:*

If melting snow is present at level the reflection of the beam can be enhanced by up to a factor of 5 due to the fact, that the backscatter cross section of the hydrometeor becomes larger because of a coverage of a thin water film on the melting snow. The rain rate is unchanged but the radar echo increases. As noted by Smith (1990) it is not so complicated to recognise a bright-band in stratiform precipitation as it is in convective. For correction of the bright-band effect, the radar must have the necessary spatial resolution to resolve the bright-band layer. This is possible for the Sindal and Rømø radars and the newly installed radar at Stevns.

### *Beam attenuation due to hydrometeors and atmosphere:*

If melting snow, hail or ground clutter is present, incorrect values for attenuation correction will be applied to the bins causing errors in the output (Collier, 1989). For example, the correction for attenuation due to hail is so unreliable that the derived rain rates cannot be used with any confidence, because for a C band radar, dry hail causes large reflectivities but smaller attenuation than rain. However, if hail less than some specific diameter is coated with a thin film of water the attenuation increases (Battan, 1973).

### *Beam power losses at range and beam filling conditions*

At increasing range the volume of the polar bin increases. The spatial distance between the Polar bins increases with range and the resampling becomes more inaccurate at longer range. At range beam filling conditions may not be fulfilled and, together with small scale variability of precipitation, the radar echo may not be representative of the precipitation conditions within the distant Polar bins. The radar measures the meteorological targets within a volume at a certain altitude above the ground surface. The problem increases with range, and for example, beam filling combined with reduced visibility can play an important role at longer ranges (Joss et al., 1995).

A rule of thumb is that closer to the radar than 100-150 km data can be used quantitatively, but at large ranges it can most often only be used qualitatively unless data are corrected for range related sources of error which can improve results to a certain extent.

### *Vertical reflectivity profile variations and beam overshooting*

At increasing range from the radar, the vertical distance between the sampling volume and the ground surface usually increases, and serious errors may arise from the variations in the vertical reflectivity profile. For example, below the radar beam the rain rate may change due to low level evaporation in a dry atmosphere, low growth in a moist atmosphere or orographic growth due to local terrain effects.

At long range, overshooting of the radar beam can cause no detection of precipitation areas, but also, missing radar samples at low altitudes may lead to a strongly underestimated rain rate. The overshooting problem is especially important in winter where the vertical extent of snowfall echoes are often less than 2 km above the ground.

When the radar beam is passing near the top of the precipitation layer the reflectivity fluctuations are not well correlated with the changes in the rain rate near the ground. In fact, Kitchen and Jackson (1993) discussed that the underestimation of rainfall accumulations at longer ranges (>100 km) is mainly caused by a steep decline in probability of detection, i.e. detection failure, and not so much by underestimation of the precipitation rate.

### *Rain gauge adjustment*

Following Joss and Waldvogel (1987) that corrections for all known systematic errors on radar data should be applied before any rain gauge adjustment. And really, something can be done to nearly all, and at least to the most important errors. On the other hand, raingauge adjustment must be done carefully because of the different nature of radar and raingauge measurements; radar data are an instant volume measure and rain gauging is a point measure of accumulated precipitation. The representativity problem can affect the comparison and has to be considered. Statistical methods for comparison can to some extent eliminate, or at least reduce, the effect of this problem.

In order to use radar for measuring rainfall intensity  $R$ , most investigators have employed an empirical expression of the general form  $Z=AR^b$  where  $A$  and  $b$  are constants. The relationship between  $Z$  and  $R$  is affected by various physical processes. Spatial and temporal variations of rain rate will affect the radar and rain gauge samples differently, and, unless treated, it will affect the raingauge adjustment. By experience it is known that the effect of not representative samples can be reduced by using many  $Z$ - $R$  values in the same rainfall system (Austin, 1987), but on the other hand many samples do not remove the scatter of the individual samples (Zawadski, 1984).

### *Variations in the drop size distribution*

The rain gauge measurements are affected by the aerodynamic error and shelter effect and, if the wind speed is high, it must be dealt with before rain gauge adjustment. The magnitude of the error on the adjustment when fixed constants in the  $Z$ - $R$  equation is used depends on how much the drop size distribution of the actual rainfall deviates from the drop size distribution assumed in the equation. In this pilot study it is the Marshall and Palmers equation, thus spatial and temporal variations in rain rate can affect the results. This argues for an adjustment based on parallel rain gauge and radar measures.

## Appendix B Tables with the overall statistics for 1998 and 1999

The verifications parameters are calculated for each of the grid point covering Jutland on monthly basis. Minimum, maximum values of all the grid points are presented below together with the average values over all grid points covering Jutland. Minimum, maximum and average values for the whole growing season is also presented.

1998	25 Obs	ME	MAE	RMSE	HR	HKSI	1998	62 Obs	ME	MAE	RMSE	HR	HKSI
MIN	Apr	-0.90	0.11	0.22	0.50	0.30	MIN	Apr	-0.79	0.09	0.21	0.53	0.39
	May	-1.05	0.07	0.14	0.48	0.22		May	-0.99	0.04	0.08	0.61	0.35
	Jun	-2.46	0.16	0.31	0.50	0.33		Jun	-1.49	0.07	0.19	0.57	0.37
	Jul	-1.26	0.26	0.47	0.35	0.17		Jul	-0.96	0.08	0.15	0.42	0.23
	Aug	-0.96	0.13	0.27	0.39	0.17		Aug	-0.93	0.03	0.06	0.42	0.28
	Sep	-1.12	0.11	0.20	0.37	0.13		Sep	-1.14	0.05	0.09	0.47	0.27
	All	-0.61	0.14	0.37	0.52	0.35		All	-0.61	0.07	0.16	0.60	0.45
MAX	Apr	1.64	2.00	4.30	0.97	0.96	MAX	Apr	1.76	1.96	3.88	1.00	1.00
	May	0.70	1.33	4.05	0.97	0.97		May	0.65	1.35	3.91	1.00	1.00
	Jun	0.83	2.85	7.15	0.97	0.95		Jun	0.82	2.21	5.00	1.00	1.00
	Jul	2.33	2.57	7.26	0.90	0.87		Jul	1.82	2.53	7.25	1.00	1.00
	Aug	0.75	1.54	3.43	1.00	1.00		Aug	0.72	1.51	3.43	1.00	1.00
	Sep	1.02	2.08	4.68	0.93	0.91		Sep	1.04	2.00	5.40	1.00	1.00
	All	0.75	1.54	3.43	0.92	0.90		All	0.54	1.31	3.15	0.96	0.93
MEAN	Apr	0.09	0.81	1.45	0.72	0.62	MEAN	Apr	0.06	0.63	1.17	0.78	0.70
	May	0.00	0.46	1.11	0.74	0.62		May	0.02	0.35	0.87	0.82	0.73
	Jun	-0.04	0.93	1.96	0.72	0.63		Jun	-0.06	0.71	1.52	0.79	0.71
	Jul	0.31	1.34	2.64	0.66	0.55		Jul	0.16	0.99	1.89	0.74	0.66
	Aug	0.03	0.75	1.44	0.68	0.56		Aug	0.07	0.59	1.14	0.75	0.66
	Sep	-0.05	0.85	1.65	0.65	0.54		Sep	0.03	0.65	1.29	0.75	0.67
	All	0.06	0.86	1.89	0.69	0.59		All	0.05	0.65	1.44	0.77	0.69

25 and 62 observations in the interpolation 1998

1998	87 Obs	ME	MAE	RMSE	HR	HKSI	1998	126 Obs	ME	MAE	RMSE	HR	HKSI
MIN	Apr	-0.77	0.08	0.15	0.50	0.35	MIN	Apr	-0.85	0.07	0.17	0.57	0.42
	May	-1.00	0.03	0.07	0.55	0.30		May	-1.04	0.02	0.04	0.55	0.28
	Jun	-1.52	0.06	0.13	0.60	0.44		Jun	-1.61	0.07	0.13	0.57	0.37
	Jul	-1.00	0.13	0.31	0.48	0.28		Jul	-0.94	0.17	0.35	0.48	0.28
	Aug	-0.99	0.02	0.05	0.45	0.28		Aug	-0.64	0.05	0.10	0.52	0.36
	Sep	-1.05	0.04	0.08	0.47	0.27		Sep	-1.06	0.04	0.07	0.47	0.28
	All	-0.61	0.08	0.21	0.62	0.50		All	-0.39	0.08	0.24	0.63	0.50
MAX	Apr	1.53	1.70	3.74	1.00	1.00	MAX	Apr	1.36	1.54	3.08	1.00	1.00
	May	0.66	1.36	4.04	1.00	1.00		May	0.64	1.39	3.99	1.00	1.00
	Jun	0.54	2.29	4.81	1.00	1.00		Jun	0.60	2.08	4.80	1.00	1.00
	Jul	1.81	2.51	7.22	1.00	1.00		Jul	1.77	2.44	7.02	1.00	1.00
	Aug	0.75	1.46	3.44	1.00	1.00		Aug	0.79	1.47	3.23	1.00	1.00
	Sep	0.80	1.83	4.91	1.00	1.00		Sep	0.78	1.61	4.63	1.00	1.00
	All	0.46	1.22	3.14	0.97	0.94		All	0.40	1.11	3.05	0.96	0.94
MEAN	Apr	0.05	0.56	1.04	0.80	0.73	MEAN	Apr	0.03	0.53	0.98	0.81	0.74
	May	0.00	0.32	0.81	0.84	0.75		May	-0.01	0.30	0.79	0.85	0.76
	Jun	-0.06	0.64	1.39	0.82	0.75		Jun	-0.07	0.61	1.33	0.82	0.76
	Jul	0.10	0.87	1.65	0.77	0.70		Jul	0.07	0.83	1.57	0.78	0.71
	Aug	0.04	0.54	1.08	0.78	0.69		Aug	0.05	0.51	1.01	0.79	0.72
	Sep	0.03	0.58	1.16	0.78	0.71		Sep	-0.01	0.53	1.08	0.79	0.72
	All	0.03	0.58	1.30	0.80	0.72		All	0.01	0.55	1.24	0.81	0.74

87 and 126 observations in the interpolation 1998



1999		25 Obs	ME	MAE	RMSE	HR	HKSI	1999		62 Obs	ME	MAE	RMSE	HR	HKSI
MIN	Apr		-0.51	0.12	0.24	0.40	0.14	MIN	Apr		-0.428	0.10	0.18	0.53	0.36
	May		-0.83	0.10	0.23	0.52	0.28		May		-0.84	0.08	0.15	0.61	0.48
	Jun		-2.18	0.29	0.46	0.27	0.07		Jun		-1.82	0.17	0.25	0.50	0.37
	Jul		-1.35	0.19	0.45	0.35	0.08		Jul		-0.95	0.12	0.24	0.52	0.32
	Aug		-2.26	0.28	0.59	0.42	0.22		Aug		-1.92	0.25	0.50	0.48	0.31
	Sep		-1.67	0.20	0.43	0.37	0.16		Sep		-1.53	0.20	0.31	0.50	0.33
	All		-0.82	0.23	0.58	0.45	0.27		All		-0.55	0.17	0.35	0.63	0.52
MAX	Apr		0.87	1.56	3.02	1.00	1.00	MAX	Apr		0.45	0.77	1.73	1.00	1.00
	May		0.69	1.55	5.36	0.94	0.92		May		0.46	1.26	5.43	1.00	1.00
	Jun		3.27	3.93	8.72	0.93	0.93		Jun		1.43	2.49	7.12	1.00	1.00
	Jul		1.46	2.92	6.97	0.97	0.95		Jul		0.89	1.55	5.10	1.00	1.00
	Aug		1.90	5.04	12.45	0.93	0.91		Aug		1.13	3.20	12.01	0.94	0.92
	Sep		2.33	3.87	7.77	0.93	0.93		Sep		1.86	2.89	6.28	1.00	1.00
	All		1.28	2.97	6.48	0.92	0.89		All		0.50	1.36	5.34	0.94	0.92
MEAN	Apr		0.05	0.56	1.13	0.69	0.59	MEAN	Apr		0.08	0.40	0.80	0.77	0.70
	May		0.04	0.55	1.26	0.73	0.65		May		0.02	0.39	0.92	0.81	0.75
	Jun		0.18	1.44	2.54	0.66	0.58		Jun		0.05	1.08	1.91	0.74	0.68
	Jul		0.03	0.95	2.10	0.73	0.62		Jul		0.07	0.70	1.59	0.80	0.72
	Aug		0.02	1.56	3.28	0.63	0.52		Aug		0.03	1.09	2.31	0.71	0.63
	Sep		0.29	1.40	2.75	0.66	0.57		Sep		0.13	0.99	2.01	0.76	0.70
	All		0.10	1.08	2.43	0.68	0.59		All		0.06	0.78	1.78	0.77	0.70

25 and 62 observations in the interpolation 1999

1999		87 Obs	ME	MAE	RMSE	HR	HKSI	1999		126 Obs	ME	MAE	RMSE	HR	HKSI
MIN	Apr		-0.44	0.09	0.17	0.53	0.40	MIN	Apr		-0.48	0.06	0.12	0.53	0.36
	May		-0.79	0.08	0.14	0.65	0.51		May		-0.78	0.06	0.10	0.65	0.50
	Jun		-1.89	0.20	0.31	0.50	0.42		Jun		-1.96	0.24	0.36	0.50	0.40
	Jul		-1.02	0.16	0.34	0.58	0.43		Jul		-0.86	0.11	0.23	0.52	0.30
	Aug		-1.85	0.32	0.58	0.52	0.36		Aug		-1.87	0.32	0.52	0.55	0.36
	Sep		-1.51	0.19	0.36	0.53	0.38		Sep		-1.64	0.14	0.30	0.57	0.41
	All		-0.56	0.20	0.39	0.67	0.55		All		-0.63	0.17	0.43	0.68	0.57
MAX	Apr		0.45	0.77	1.76	1.00	1.00	MAX	Apr		0.47	0.76	1.85	1.00	1.00
	May		0.41	1.32	5.49	1.00	1.00		May		0.42	1.26	5.36	1.00	1.00
	Jun		1.33	2.61	7.44	0.97	0.97		Jun		1.20	2.73	7.69	0.97	0.96
	Jul		0.75	1.56	5.01	1.00	1.00		Jul		0.80	1.57	4.67	1.00	1.00
	Aug		0.87	3.04	12.03	0.97	0.95		Aug		0.85	3.07	12.25	0.94	0.92
	Sep		1.60	2.12	4.94	1.00	1.00		Sep		1.45	1.92	4.32	1.00	1.00
	All		0.51	1.31	5.34	0.93	0.90		All		0.46	1.37	5.41	0.91	0.89
MEAN	Apr		0.06	0.38	0.77	0.79	0.72	MEAN	Apr		0.06	0.38	0.77	0.79	0.72
	May		0.01	0.37	0.87	0.83	0.77		May		0.02	0.37	0.87	0.83	0.78
	Jun		0.04	1.04	1.84	0.75	0.69		Jun		-0.03	1.04	1.86	0.75	0.70
	Jul		0.05	0.67	1.52	0.81	0.74		Jul		0.04	0.64	1.46	0.82	0.75
	Aug		-0.02	1.02	2.13	0.72	0.64		Aug		-0.04	1.00	2.11	0.72	0.65
	Sep		0.09	0.93	1.89	0.78	0.72		Sep		0.03	0.90	1.82	0.79	0.73
	All		0.04	0.73	1.68	0.78	0.72		All		0.01	0.72	1.66	0.78	0.72

87 and 126 observations in the interpolation 1999



No calibration							No calibration, anaprob days = 0						
1998		ME	MAE	RMSE	HR	HKSI	1998		ME	MAE	RMSE	HR	HKSI
MIN	Apr	-1.94	0.63	0.97	0.23	-0.05	MIN	Apr	-1.94	0.63	0.97	0.23	-0.05
	May	-0.92	0.19	0.38	0.19	-0.14		May	-0.92	0.19	0.38	0.26	-0.08
	Jun	-3.08	0.32	0.58	0.33	0.08		Jun	-3.08	0.32	0.58	0.33	0.08
	Jul	-2.05	0.49	0.78	0.30	0.09		Jul	-2.05	0.49	0.78	0.30	0.09
	Aug	-1.87	0.47	0.81	0.27	0.02		Aug	-1.87	0.47	0.81	0.27	0.02
	Sep	-1.92	0.36	0.60	0.29	0.00		Sep	-1.92	0.36	0.60	0.29	0.00
All	-1.33	0.88	1.62	0.45	0.15	All	-1.33	0.88	1.62	0.45	0.16		
MAX	Apr	2.56	3.78	8.57	0.73	0.64	MAX	Apr	2.56	3.78	8.57	0.73	0.64
	May	7.53	8.26	22.31	0.94	0.82		May	7.31	8.04	22.28	0.94	0.82
	Jun	2.72	4.09	14.25	0.85	0.80		Jun	2.72	4.09	14.25	0.85	0.80
	Jul	1.26	3.43	6.24	0.83	0.77		Jul	1.26	3.43	6.24	0.83	0.77
	Aug	2.10	3.37	9.71	0.81	0.69		Aug	2.10	3.37	9.71	0.81	0.69
	Sep	0.47	2.64	5.93	0.88	0.76		Sep	0.47	2.64	5.93	0.88	0.76
All	1.55	3.06	10.37	0.71	0.55	All	1.42	2.93	10.36	0.71	0.56		
MEAN	Apr	-0.14	1.66	3.08	0.51	0.34	MEAN	Apr	-0.14	1.66	3.08	0.51	0.34
	May	0.50	1.23	3.00	0.62	0.35		May	0.34	1.07	2.59	0.65	0.37
	Jun	-0.05	1.36	2.98	0.65	0.50		Jun	-0.05	1.36	2.98	0.65	0.50
	Jul	-0.57	1.48	2.73	0.58	0.44		Jul	-0.57	1.48	2.73	0.58	0.44
	Aug	-0.55	1.35	2.69	0.56	0.35		Aug	-0.55	1.35	2.69	0.56	0.35
	Sep	-0.72	1.05	2.09	0.64	0.43		Sep	-0.72	1.05	2.09	0.64	0.43
All	-0.23	1.36	3.07	0.59	0.40	All	-0.26	1.34	2.97	0.60	0.40		

Radar derived precipitation 1998, original phase I, original phase I with anaprop correction

Calibrated, anaprob days = 0							Calibrated with factor						
1998		ME	MAE	RMSE	HR	HKSI	1998		ME	MAE	RMSE	HR	HKSI
MIN	Apr	-2.18	0.51	0.75	0.26	-0.07	MIN	Apr	-2.28	0.53	0.77	0.23	-0.13
	May	-0.88	0.22	0.39	0.31	0.13		May	-1.25	0.24	0.41	0.29	0.09
	Jun	-3.04	0.31	0.49	0.37	0.22		Jun	-3.28	0.33	0.50	0.40	0.24
	Jul	-1.88	0.47	0.66	0.40	0.16		Jul	-1.95	0.49	0.67	0.41	0.17
	Aug	-1.10	0.24	0.55	0.38	0.18		Aug	-1.20	0.26	0.54	0.42	0.20
	Sep	-1.73	0.29	0.57	0.42	0.17		Sep	-1.89	0.31	0.59	0.41	0.18
All	-1.27	0.69	1.25	0.42	0.26	All	-1.41	0.72	1.30	0.44	0.27		
MAX	Apr	2.03	2.47	6.24	0.87	0.84	MAX	Apr	2.13	2.59	6.38	0.86	0.83
	May	12.12	12.19	31.82	0.97	0.95		May	7.18	7.27	22.76	1.00	1.00
	Jun	2.63	3.38	13.06	0.93	0.91		Jun	2.84	3.65	13.57	0.92	0.93
	Jul	1.74	2.59	5.67	0.93	0.90		Jul	1.80	2.66	5.77	0.93	0.90
	Aug	2.61	3.51	10.25	0.92	0.91		Aug	1.82	2.21	3.78	1.00	1.00
	Sep	1.32	2.69	7.64	0.92	0.91		Sep	1.44	2.93	7.98	0.95	0.95
All	2.73	3.48	14.16	0.79	0.70	All	1.33	2.15	9.04	0.80	0.72		
MEAN	Apr	-0.20	1.27	2.35	0.62	0.48	MEAN	Apr	-0.23	1.30	2.38	0.62	0.48
	May	0.53	1.07	2.65	0.65	0.54		May	0.19	0.93	2.16	0.66	0.54
	Jun	-0.07	1.15	2.47	0.69	0.58		Jun	-0.14	1.18	2.42	0.69	0.58
	Jul	0.00	1.23	2.40	0.68	0.56		Jul	0.00	1.27	2.44	0.67	0.56
	Aug	0.02	0.97	2.00	0.66	0.53		Aug	-0.12	0.90	1.77	0.70	0.58
	Sep	-0.06	0.89	1.89	0.74	0.63		Sep	-0.07	0.97	1.97	0.73	0.62
All	0.05	1.10	2.60	0.67	0.55	All	-0.06	1.10	2.44	0.68	0.56		

Radar derived precipitation 1998, adjusted radar and anaprop correction, factor calibration

		No calibration							No calibration, anaprob days = 0				
1999		ME	MAE	RMSE	HR	HKSI	1999		ME	MAE	RMSE	HR	HKSI
MIN	Apr	-2.16	0.20	0.36	0.29	-0.06	MIN	Apr	-2.16	0.20	0.36	0.38	0.00
	May	-1.51	0.26	0.48	0.28	-0.01		May	-1.59	0.25	0.40	0.44	0.08
	Jun	-3.60	0.64	1.03	0.38	0.14		Jun	-3.60	0.64	1.03	0.38	0.14
	Jul	-3.29	0.46	0.91	0.19	-0.01		Jul	-3.32	0.44	0.91	0.42	0.07
	Aug	-5.25	0.52	0.84	0.19	-0.08		Aug	-5.25	0.51	0.84	0.24	-0.03
	Sep	-3.61	0.54	1.04	0.29	0.12		Sep	-3.62	0.54	1.04	0.43	0.16
	All	-2.77	0.61	1.24	0.37	0.09		All	-2.78	0.60	1.24	0.48	0.17
MAX	Apr	5.15	5.32	18.05	0.86	0.73	MAX	Apr	3.98	4.15	14.04	0.86	0.77
	May	2.70	4.72	10.30	0.96	0.91		May	1.10	3.59	9.82	0.96	0.91
	Jun	1.75	4.11	9.60	0.92	0.88		Jun	1.58	4.11	9.60	0.92	0.88
	Jul	7.73	8.88	22.54	0.77	0.65		Jul	2.52	4.32	10.52	0.85	0.74
	Aug	7.07	8.41	20.69	0.82	0.74		Aug	5.75	6.75	20.62	0.86	0.79
	Sep	5.77	7.31	13.45	0.86	0.83		Sep	5.29	6.79	13.36	0.90	0.89
	All	3.68	5.13	12.87	0.78	0.64		All	2.17	3.46	10.27	0.81	0.67
MEAN	Apr	-0.03	1.22	2.71	0.58	0.34	MEAN	Apr	-0.23	1.02	2.15	0.61	0.37
	May	-0.11	1.13	2.53	0.64	0.42		May	-0.22	1.02	2.34	0.68	0.46
	Jun	-0.28	1.55	2.90	0.65	0.53		Jun	-0.30	1.53	2.89	0.67	0.54
	Jul	0.43	2.25	4.87	0.54	0.35		Jul	-0.41	1.41	3.29	0.67	0.48
	Aug	0.09	2.26	4.36	0.53	0.37		Aug	-0.12	2.05	4.09	0.56	0.41
	Sep	-0.23	2.16	3.95	0.61	0.47		Sep	-0.34	2.06	3.85	0.65	0.52
	All	-0.01	1.76	3.95	0.59	0.41		All	-0.27	1.50	3.40	0.64	0.46

Radar derived precipitation 1999, original phase I, original phase I with anaprop correction

		Calibrated, anaprob days = 0							Calibrated with factor				
1999		ME	MAE	RMSE	HR	HKSI	1999		ME	MAE	RMSE	HR	HKSI
MIN	Apr	-1.30	0.20	0.38	0.33	0.06	MIN	Apr	-1.52	0.23	0.41	0.28	0.04
	May	-1.08	0.20	0.44	0.52	0.24		May	-1.29	0.25	0.50	0.35	0.04
	Jun	-2.51	0.37	0.61	0.50	0.24		Jun	-2.87	0.42	0.65	0.33	0.19
	Jul	-3.12	0.32	0.56	0.46	0.21		Jul	-4.28	0.43	0.66	0.32	0.14
	Aug	-4.84	0.45	0.74	0.36	0.15		Aug	-5.94	0.47	0.77	0.33	0.15
	Sep	-3.29	0.47	0.83	0.38	0.24		Sep	-3.83	0.53	0.86	0.22	0.12
	All	-2.43	0.45	0.95	0.51	0.32		All	-2.97	0.53	1.05	0.40	0.27
MAX	Apr	6.45	6.87	15.43	0.95	0.92	MAX	Apr	3.66	4.15	9.13	0.94	0.93
	May	1.63	2.68	7.40	1.00	1.00		May	2.04	3.34	8.28	1.00	1.00
	Jun	1.75	2.68	6.83	1.00	1.00		Jun	2.00	3.06	7.30	1.00	1.00
	Jul	2.90	3.69	13.16	0.96	0.95		Jul	3.97	5.05	15.40	0.95	0.94
	Aug	7.18	7.89	24.73	0.86	0.83		Aug	4.70	6.51	16.78	1.00	1.00
	Sep	10.55	10.94	38.93	0.95	0.96		Sep	5.16	5.38	10.08	1.00	1.00
	All	2.93	3.74	16.30	0.84	0.78		All	1.98	3.27	7.30	0.82	0.76
MEAN	Apr	0.10	0.95	2.00	0.65	0.51	MEAN	Apr	-0.04	0.95	1.89	0.65	0.52
	May	0.13	0.81	1.81	0.76	0.67		May	0.15	1.01	2.01	0.69	0.58
	Jun	-0.04	1.07	2.07	0.76	0.68		Jun	-0.04	1.22	2.21	0.72	0.64
	Jul	-0.03	0.96	2.16	0.74	0.64		Jul	-0.12	1.22	2.32	0.68	0.57
	Aug	0.64	2.07	4.32	0.60	0.49		Aug	-0.07	1.67	3.07	0.65	0.55
	Sep	0.65	1.83	3.52	0.70	0.63		Sep	0.56	1.95	3.41	0.69	0.61
	All	0.22	1.26	3.01	0.71	0.60		All	0.07	1.33	2.74	0.68	0.58

Radar derived precipitation 1998, adjusted radar and anaprop correction, factor calibration

## Appendix C Contingency tables for 25 observations in the interpolation 1998

AMIS		KLIMA					mm nedbør
		0	0.05	2	6	10	
		0.05	2	6	10	100	
0	0.05	1916	342	4	0	0	
	0.05	2	1165	2857	343	4	1
	2	6	14	513	2306	258	16
	6	10	0	35	238	458	79
	10	100	0	0	31	80	428

mm nedbør

Kontingenstabel for 1/4-98 - 30/4-98

AMIS		KLIMA					mm nedbør
		0	0.05	2	6	10	
		0.05	2	6	10	100	
0	0.05	5550	303	17	7	5	
	0.05	2	1732	1707	293	21	0
	2	6	18	241	813	123	34
	6	10	10	17	122	268	71
	10	100	0	0	10	24	70

mm nedbør

Kontingenstabel for 1/5-98 - 31/5-98

AMIS		KLIMA					mm nedbør
		0	0.05	2	6	10	
		0.05	2	6	10	100	
0	0.05	3649	210	3	0	0	
	0.05	2	1223	2412	370	16	1
	2	6	25	389	1001	226	41
	6	10	0	23	263	375	151
	10	100	0	1	23	116	582

mm nedbør

Kontingenstabel for 1/6-98 - 30/6-98

AMIS		KLIMA					mm nedbør
		0	0.05	2	6	10	
		0.05	2	6	10	100	
0	0.05	1625	298	7	0	0	
	0.05	2	1261	2856	504	20	2
	2	6	29	522	1575	230	51
	6	10	1	41	402	606	191
	10	100	0	21	86	255	887

mm nedbør

Kontingenstabel for 1/7-98 - 31/7-98

AMIS		KLIMA					mm nedbør
		0	0.05	2	6	10	
		0.05	2	6	10	100	
0	0.05	2529	274	4	0	0	
	0.05	2	1795	3258	574	29	9
	2	6	21	359	1118	126	9
	6	10	2	12	180	286	108
	10	100	0	1	20	137	615

mm nedbør

Kontingenstabel for 1/8-98 - 31/8-98

AMIS		KLIMA					mm nedbør
		0	0.05	2	6	10	
		0.05	2	6	10	100	
0	0.05	3062	337	18	5	0	
	0.05	2	1815	2163	468	32	3
	2	6	9	379	1187	180	57
	6	10	1	22	215	310	177
	10	100	0	0	11	150	485

mm nedbør

Kontingenstabel for 1/9-98 - 30/9-98

## Appendix D Contingency tables for 62 observations in the interpolation 1998

KLIMA		0	0.05	2	6	10	mm nedbør
AMIS		0.05	2	6	10	100	
0	0.05	2307	358	5	1	0	
0.05	2	790	3030	339	3	0	
2	6	1	345	2335	200	8	
6	10	0	13	228	539	73	
10	100	0	0	15	58	443	

mm nedbør

Kontingenstabel for 1/4-98 - 30/4-98

KLIMA		0	0.05	2	6	10	mm nedbør
AMIS		0.05	2	6	10	100	
0	0.05	6262	260	2	0	0	
0.05	2	1050	1780	199	13	5	
2	6	2	226	944	108	15	
6	10	0	4	105	283	54	
10	100	0	0	5	39	106	

mm nedbør

Kontingenstabel for 1/5-98 - 31/5-98

KLIMA		0	0.05	2	6	10	mm nedbør
AMIS		0.05	2	6	10	100	
0	0.05	4082	243	8	0	0	
0.05	2	811	2479	302	15	1	
2	6	4	305	1162	192	15	
6	10	0	7	176	424	146	
10	100	0	1	12	102	613	

mm nedbør

Kontingenstabel for 1/6-98 - 30/6-98

KLIMA		0	0.05	2	6	10	mm nedbør
AMIS		0.05	2	6	10	100	
0	0.05	2002	252	2	0	0	
0.05	2	905	3040	337	7	2	
2	6	9	420	1874	240	39	
6	10	0	22	315	650	150	
10	100	0	4	45	214	940	

mm nedbør

Kontingenstabel for 1/7-98 - 31/7-98

KLIMA		0	0.05	2	6	10	mm nedbør
AMIS		0.05	2	6	10	100	
0	0.05	3052	302	5	0	0	
0.05	2	1289	3207	330	11	0	
2	6	6	392	1379	125	12	
6	10	0	3	170	345	102	
10	100	0	0	14	97	627	

mm nedbør

Kontingenstabel for 1/8-98 - 31/8-98

KLIMA		0	0.05	2	6	10	mm nedbør
AMIS		0.05	2	6	10	100	
0	0.05	3778	296	1	0	0	
0.05	2	1105	2227	335	12	1	
2	6	8	362	1390	161	18	
6	10	0	16	163	364	129	
10	100	0	0	8	140	574	

mm nedbør

Kontingenstabel for 1/9-98 - 30/9-98

## Appendix E Contingency tables for 87 observations in the interpolation 1998

KLIMA		0	0.05	2	6	10	mm nedbør
AMIS		0.05	2	6	10	100	
0	0.05	2413	344	3	0	0	
0.05	2	685	3064	283	2	0	
2	6	1	337	2409	174	7	
6	10	0	4	219	583	71	
10	100	0	0	8	42	446	

mm nedbør

Kontingenstabel for 1/4-98 - 30/4-98

KLIMA		0	0.05	2	6	10	mm nedbør
AMIS		0.05	2	6	10	100	
0	0.05	6408	259	3	0	0	
0.05	2	907	1818	200	10	5	
2	6	1	188	957	109	18	
6	10	0	4	90	289	38	
10	100	0	0	5	35	119	

mm nedbør

Kontingenstabel for 1/5-98 - 31/5-98

KLIMA		0	0.05	2	6	10	mm nedbør
AMIS		0.05	2	6	10	100	
0	0.05	4223	235	5	0	0	
0.05	2	672	2553	291	16	1	
2	6	2	244	1218	197	11	
6	10	0	3	134	414	119	
10	100	0	0	11	106	644	

mm nedbør

Kontingenstabel for 1/6-98 - 30/6-98

KLIMA		0	0.05	2	6	10	mm nedbør
AMIS		0.05	2	6	10	100	
0	0.05	2162	266	3	0	0	
0.05	2	748	3096	338	4	2	
2	6	6	358	1920	206	33	
6	10	0	17	279	693	138	
10	100	0	1	33	208	958	

mm nedbør

Kontingenstabel for 1/7-98 - 31/7-98

KLIMA		0	0.05	2	6	10	mm nedbør
AMIS		0.05	2	6	10	100	
0	0.05	3289	343	3	0	0	
0.05	2	1052	3226	319	6	0	
2	6	6	333	1423	138	11	
6	10	0	3	141	343	109	
10	100	0	0	12	91	621	

mm nedbør

Kontingenstabel for 1/8-98 - 31/8-98

KLIMA		0	0.05	2	6	10	mm nedbør
AMIS		0.05	2	6	10	100	
0	0.05	3942	314	0	0	0	
0.05	2	942	2274	294	7	0	
2	6	7	300	1448	140	16	
6	10	0	13	147	407	111	
10	100	0	0	11	123	595	

mm nedbør

Kontingenstabel for 1/9-98 - 30/9-98

## Appendix F Contingency tables for 126 observations in the interpolation 1998

AMIS		KLIMA		0	0.05	2	6	10	mm nedbør
		0.05	2	6	10	100			
0	0.05	2390	337	3	0	0			
0.05	2	708	3114	295	3	0			
2	6	1	294	2414	167	9			
6	10	0	2	205	578	59			
10	100	0	0	5	52	456			

mm nedbør

Kontingenstabel for 1/4-98 - 30/4-98

AMIS		KLIMA		0	0.05	2	6	10	mm nedbør
		0.05	2	6	10	100			
0	0.05	6525	254	3	0	0			
0.05	2	790	1818	171	6	5			
2	6	0	196	988	108	21			
6	10	0	3	90	298	33			
10	100	0	0	3	31	121			

mm nedbør

Kontingenstabel for 1/5-98 - 31/5-98

AMIS		KLIMA		0	0.05	2	6	10	mm nedbør
		0.05	2	6	10	100			
0	0.05	4267	229	2	0	0			
0.05	2	630	2588	310	12	0			
2	6	0	216	1214	199	16			
6	10	0	2	123	420	106			
10	100	0	0	10	102	653			

mm nedbør

Kontingenstabel for 1/6-98 - 30/6-98

AMIS		KLIMA		0	0.05	2	6	10	mm nedbør
		0.05	2	6	10	100			
0	0.05	2230	278	2	0	0			
0.05	2	682	3108	326	4	1			
2	6	4	333	1939	209	18			
6	10	0	18	277	702	143			
10	100	0	1	30	196	969			

mm nedbør

Kontingenstabel for 1/7-98 - 31/7-98

AMIS		KLIMA		0	0.05	2	6	10	mm nedbør
		0.05	2	6	10	100			
0	0.05	3392	296	1	0	0			
0.05	2	947	3290	316	8	0			
2	6	8	314	1441	134	5			
6	10	0	4	126	351	102			
10	100	0	1	14	85	634			

mm nedbør

Kontingenstabel for 1/8-98 - 31/8-98

AMIS		KLIMA		0	0.05	2	6	10	mm nedbør
		0.05	2	6	10	100			
0	0.05	3996	292	0	0	0			
0.05	2	895	2311	280	4	1			
2	6	2	295	1476	139	11			
6	10	0	4	134	417	122			
10	100	0	0	6	117	588			

mm nedbør

Kontingenstabel for 1/9-98 - 30/9-98



# Appendix G Contingency tables for 25 observations in the interpolation 1999

KLIMA		0	0.05	2	6	10	mm nedbør
AMIS		0.05	2	6	10	100	
0	0.05	3851	189	1	0	0	
0.05	2	1836	2482	135	3	0	
2	6	6	307	1130	213	14	
6	10	0	11	158	373	136	
10	100	0	2	7	67	177	

mm nedbør

Kontingenstabel for 1/4-98 - 30/4-98

KLIMA		0	0.05	2	6	10	mm nedbør
AMIS		0.05	2	6	10	100	
0	0.05	5154	88	4	3	0	
0.05	2	1628	1981	181	7	0	
2	6	4	361	1072	147	22	
6	10	0	1	92	249	91	
10	100	0	0	2	66	308	

mm nedbør

Kontingenstabel for 1/5-98 - 31/5-98

KLIMA		0	0.05	2	6	10	mm nedbør
AMIS		0.05	2	6	10	100	
0	0.05	2865	177	8	3	0	
0.05	2	1076	1380	274	18	9	
2	6	7	334	1205	348	63	
6	10	0	18	454	820	246	
10	100	0	1	27	324	1441	

mm nedbør

Kontingenstabel for 1/6-98 - 30/6-98

KLIMA		0	0.05	2	6	10	mm nedbør
AMIS		0.05	2	6	10	100	
0	0.05	4962	232	1	0	0	
0.05	2	1043	1954	419	22	12	
2	6	2	332	1014	191	39	
6	10	0	39	274	221	135	
10	100	0	9	69	141	357	

mm nedbør

Kontingenstabel for 1/7-98 - 31/7-98

KLIMA		0	0.05	2	6	10	mm nedbør
AMIS		0.05	2	6	10	100	
0	0.05	4404	265	12	3	3	
0.05	2	1238	1322	427	39	18	
2	6	49	414	934	311	127	
6	10	1	42	194	425	271	
10	100	0	44	131	197	554	

mm nedbør

Kontingenstabel for 1/8-98 - 31/8-98

KLIMA		0	0.05	2	6	10	mm nedbør
AMIS		0.05	2	6	10	100	
0	0.05	4015	160	3	0	0	
0.05	2	1445	1402	222	11	8	
2	6	7	298	789	199	32	
6	10	0	15	318	401	196	
10	100	0	2	125	378	1064	

mm nedbør

Kontingenstabel for 1/9-98 - 30/9-98

## Appendix H Contingency tables for 62 observations in the interpolation 1999

KLIMA		0	0.05	2	6	10	mm nedbør
AMIS		0.05	2	6	10	100	
0	0.05	4617	220	1	0	0	
0.05	2	1075	2581	150	3	0	
2	6	2	182	1120	147	6	
6	10	0	6	154	418	73	
10	100	0	2	6	88	248	

mm nedbør

**Kontingenstabel for 1/4-98 - 30/4-98**

KLIMA		0	0.05	2	6	10	mm nedbør
AMIS		0.05	2	6	10	100	
0	0.05	5926	113	4	2	0	
0.05	2	867	2088	171	1	0	
2	6	2	229	1078	116	2	
6	10	0	1	93	270	51	
10	100	0	0	4	82	368	

mm nedbør

**Kontingenstabel for 1/5-98 - 31/5-98**

KLIMA		0	0.05	2	6	10	mm nedbør
AMIS		0.05	2	6	10	100	
0	0.05	3310	163	7	3	0	
0.05	2	632	1432	220	13	6	
2	6	8	307	1391	271	43	
6	10	0	7	334	974	237	
10	100	0	1	15	252	1473	

mm nedbør

**Kontingenstabel for 1/6-98 - 30/6-98**

KLIMA		0	0.05	2	6	10	mm nedbør
AMIS		0.05	2	6	10	100	
0	0.05	5418	199	3	2	1	
0.05	2	587	2033	303	14	9	
2	6	3	321	1203	160	23	
6	10	0	8	226	263	102	
10	100	0	5	42	136	408	

mm nedbør

**Kontingenstabel for 1/7-98 - 31/7-98**

KLIMA		0	0.05	2	6	10	mm nedbør
AMIS		0.05	2	6	10	100	
0	0.05	4946	265	16	2	3	
0.05	2	737	1455	363	40	10	
2	6	17	341	1013	225	58	
6	10	0	27	221	496	198	
10	100	0	13	85	212	704	

mm nedbør

**Kontingenstabel for 1/8-98 - 31/8-98**

KLIMA		0	0.05	2	6	10	mm nedbør
AMIS		0.05	2	6	10	100	
0	0.05	4750	155	4	0	0	
0.05	2	725	1537	174	8	5	
2	6	1	177	921	200	33	
6	10	0	7	301	512	141	
10	100	0	1	57	269	1121	

mm nedbør

**Kontingenstabel for 1/9-98 - 30/9-98**

# Appendix I Contingency tables for 87 observations in the interpolation 1999

KLIMA		0	0.05	2	6	10	mm nedbør
AMIS		0.05	2	6	10	100	
0	0.05	4806	242	1	0	0	
0.05	2	886	2572	148	4	0	
2	6	1	165	1124	132	6	
6	10	0	6	152	431	69	
10	100	0	2	6	89	252	

mm nedbør

**Kontingenstabel for 1/4-98 - 30/4-98**

KLIMA		0	0.05	2	6	10	mm nedbør
AMIS		0.05	2	6	10	100	
0	0.05	6080	130	1	0	0	
0.05	2	712	2118	179	3	0	
2	6	1	183	1072	100	3	
6	10	0	0	91	294	56	
10	100	0	0	5	72	362	

mm nedbør

**Kontingenstabel for 1/5-98 - 31/5-98**

KLIMA		0	0.05	2	6	10	mm nedbør
AMIS		0.05	2	6	10	100	
0	0.05	3421	182	2	1	0	
0.05	2	526	1450	174	8	3	
2	6	2	271	1478	251	34	
6	10	0	7	298	999	223	
10	100	0	0	14	254	1499	

mm nedbør

**Kontingenstabel for 1/6-98 - 30/6-98**

KLIMA		0	0.05	2	6	10	mm nedbør
AMIS		0.05	2	6	10	100	
0	0.05	5522	198	0	0	0	
0.05	2	481	2057	283	13	9	
2	6	4	300	1265	159	24	
6	10	0	7	203	294	95	
10	100	0	4	26	109	415	

mm nedbør

**Kontingenstabel for 1/7-98 - 31/7-98**

KLIMA		0	0.05	2	6	10	mm nedbør
AMIS		0.05	2	6	10	100	
0	0.05	5034	286	18	1	0	
0.05	2	652	1500	338	37	12	
2	6	12	282	1064	212	56	
6	10	1	25	218	532	198	
10	100	0	8	60	193	707	

mm nedbør

**Kontingenstabel for 1/8-98 - 31/8-98**

KLIMA		0	0.05	2	6	10	mm nedbør
AMIS		0.05	2	6	10	100	
0	0.05	4931	169	4	0	0	
0.05	2	544	1532	173	8	4	
2	6	1	169	990	199	26	
6	10	0	5	257	560	153	
10	100	0	2	33	222	1117	

mm nedbør

**Kontingenstabel for 1/9-98 - 30/9-98**

## Appendix J Contingency tables for 126 observations in the interpolation 1999

KLIMA		0	0.05	2	6	10	mm nedbør
AMIS		0.05	2	6	10	100	
0	0.05	4861	236	1	0	0	
0.05	2	826	2580	146	4	0	
2	6	7	167	1137	120	2	
6	10	0	7	140	454	72	
10	100	0	0	7	78	253	

mm nedbør

**Kontingenstabel for 1/4-98 - 30/4-98**

KLIMA		0	0.05	2	6	10	mm nedbør
AMIS		0.05	2	6	10	100	
0	0.05	6160	128	0	0	0	
0.05	2	632	2112	208	3	0	
2	6	3	189	1046	96	4	
6	10	0	2	94	297	54	
10	100	0	0	3	76	363	

mm nedbør

**Kontingenstabel for 1/5-98 - 31/5-98**

KLIMA		0	0.05	2	6	10	mm nedbør
AMIS		0.05	2	6	10	100	
0	0.05	3532	172	2	2	0	
0.05	2	414	1476	177	10	4	
2	6	4	247	1508	288	35	
6	10	0	15	262	962	209	
10	100	0	0	17	251	1511	

mm nedbør

**Kontingenstabel for 1/6-98 - 30/6-98**

KLIMA		0	0.05	2	6	10	mm nedbør
AMIS		0.05	2	6	10	100	
0	0.05	5579	186	0	0	0	
0.05	2	427	2087	292	12	9	
2	6	3	283	1276	145	13	
6	10	0	9	186	302	93	
10	100	0	1	23	116	428	

mm nedbør

**Kontingenstabel for 1/7-98 - 31/7-98**

KLIMA		0	0.05	2	6	10	mm nedbør
AMIS		0.05	2	6	10	100	
0	0.05	5147	287	17	1	0	
0.05	2	541	1540	341	40	15	
2	6	13	270	1070	194	46	
6	10	1	17	220	553	191	
10	100	0	8	48	187	721	

mm nedbør

**Kontingenstabel for 1/8-98 - 31/8-98**

KLIMA		0	0.05	2	6	10	mm nedbør
AMIS		0.05	2	6	10	100	
0	0.05	4980	172	4	0	0	
0.05	2	491	1540	165	8	5	
2	6	1	157	1013	198	21	
6	10	0	7	245	585	174	
10	100	0	1	30	198	1100	

mm nedbør

**Kontingenstabel for 1/9-98 - 30/9-98**

